

# Strontium Isotope Composition of Rocks and Ores of the Porozhinsk Deposit (Yenisei Ridge, Krasnoyarsk Region)

V. N. Kuleshov<sup>a,\*</sup>, M. I. Bujakaite<sup>a,\*\*</sup>, N. B. Kuznetsov<sup>a, b,\*\*\*</sup>, and L. I. Sviridov<sup>c,\*\*\*\*</sup>

<sup>a</sup> Geological Institute, Russian Academy of Sciences, Moscow, 119017 Russia

<sup>b</sup> Institute of the Earth's Crust, Siberian Branch, Russian Academy of Sciences, Irkutsk, 664033 Russia

<sup>c</sup> Siberian Federal University (Institute of Oil and Gas), Krasnoyarsk, 660041 Russia

\*e-mail: vnkuleshov@mail.ru

\*\*e-mail: buyakaite@ginras.ru

\*\*\*e-mail: kouzniebor@mail.ru

\*\*\*\*e-mail: Sviridov@sfu-kras.ru

Received March 17, 2021; revised June 5, 2021; accepted April 29, 2022

**Abstract**—Wide variations of  $^{87}\text{Sr}/^{86}\text{Sr}$  (0.70825–0.70924) have been established at the Porozhinsk deposit in manganese ores and carbonates ascribed to the Pod'emska Formation. These data, together with variations in the carbon ( $\delta^{13}\text{C} = -14.6\text{...}2.0\text{‰}$ , PDB) and oxygen ( $\delta^{18}\text{O} = 19.4\text{...}28.3\text{‰}$ , SMOW) isotope composition indicate different conditions of the formation of the studied rocks. The  $^{87}\text{Sr}/^{86}\text{Sr}$  values in the studied dolomites of the Porozhinsk deposit are much higher than those of carbonate rocks (dolomites, limestones) of the Pod'emska Formation from the Chapa River section. The position of the  $^{87}\text{Sr}/^{86}\text{Sr}$  values of dolomites from the Porozhinsk deposit on the secular  $^{87}\text{Sr}/^{86}\text{Sr}$  variation curve for Late Proterozoic ocean (Kuznetsov et al., 2014) suggests that the carbonate rocks attributed to the Pod'emska Formation at the Porozhinsk deposit have younger age than carbonates of the Pod'emska Formation from the Chapa River section. The Mn/Sr values usually taken as a criterion for the degree of secondary alteration of carbonates (in interpreting  $^{87}\text{Sr}/^{86}\text{Sr}$  variations and discussing the suitability of the material for chemostratigraphic constructions) are not suitable for rocks formed in manganese ore sedimentation basins.

**Keywords:** manganese deposit, manganese ores, isotope geochemistry, strontium, dolomites, Neoproterozoic, Yenisei Ridge

**DOI:** 10.1134/S0024490222050029

## INTRODUCTION

The Porozhinsk manganese deposit is located in the southern Turukhansk area of the Krasnoyarsk region, in the northwestern Yenisei Ridge, 650 km north of Krasnoyarsk (Fig. 1). This deposit is one of the Russia's largest manganese deposits. Its total reserves are 29.46 Mt (*Gosudarstvennyi ...*, 2019). It is restricted to the Vorogovka trough, which was initiated in the Neoproterozoic (Mstislavsky and Potkonen, 1990; Sovetov and Le Heron, 2016; Vishnevskaya et al., 2017).

The aureoles of manganese mineralization within the Vorogovka trough were discovered in 1974. During the prospecting for manganese (1976–1982) and preliminary exploration in 1982–1984, several project sectors were distinguished, including the Mokhovoi and Porozhinsk sectors. As has been already mentioned (Kuleshov, 2018; Kuleshov et al., 2021), an enormous amount of factual material has been accumulated on the geology, mineralogy, and geochemistry of manganese ores of the deposit. At the same time, some features of rocks of the Porozhinsk deposit, which are important for the interpretation of timing

and conditions of its formation, have been insufficiently studied. In particular, the strontium isotope study ( $^{87}\text{Sr}/^{86}\text{Sr}$ ) of this deposit has not been carried out yet.

This work reports new data on strontium isotope composition of manganese carbonates from karst depressions and host dolomites, which are ascribed to the Porozhinsk and Mokhovoi sectors to the Pod'emska Formation of the Upper Neoproterozoic Chapa Group of the Vorogovka Trough. The  $^{87}\text{Sr}/^{86}\text{Sr}$  distribution in combination with carbon ( $\delta^{13}\text{C}$ ) and oxygen ( $\delta^{18}\text{O}$ ) isotope data and abundance of some chemical components (Rb, Sr, Mg/Ca,  $\text{SiO}_2$ ,  $\text{Fe}_3\text{O}_4$ , and others) made it possible to decipher the genesis of rocks and ores of the considered deposit and to roughly estimate their age and age of the ore-bearing carbonate sequence.

## GENERAL GEOLOGY

The geological structure of the Porozhinsk deposit in general was well studied. The detailed prospecting and exploration of manganese ore lodes with calcu-

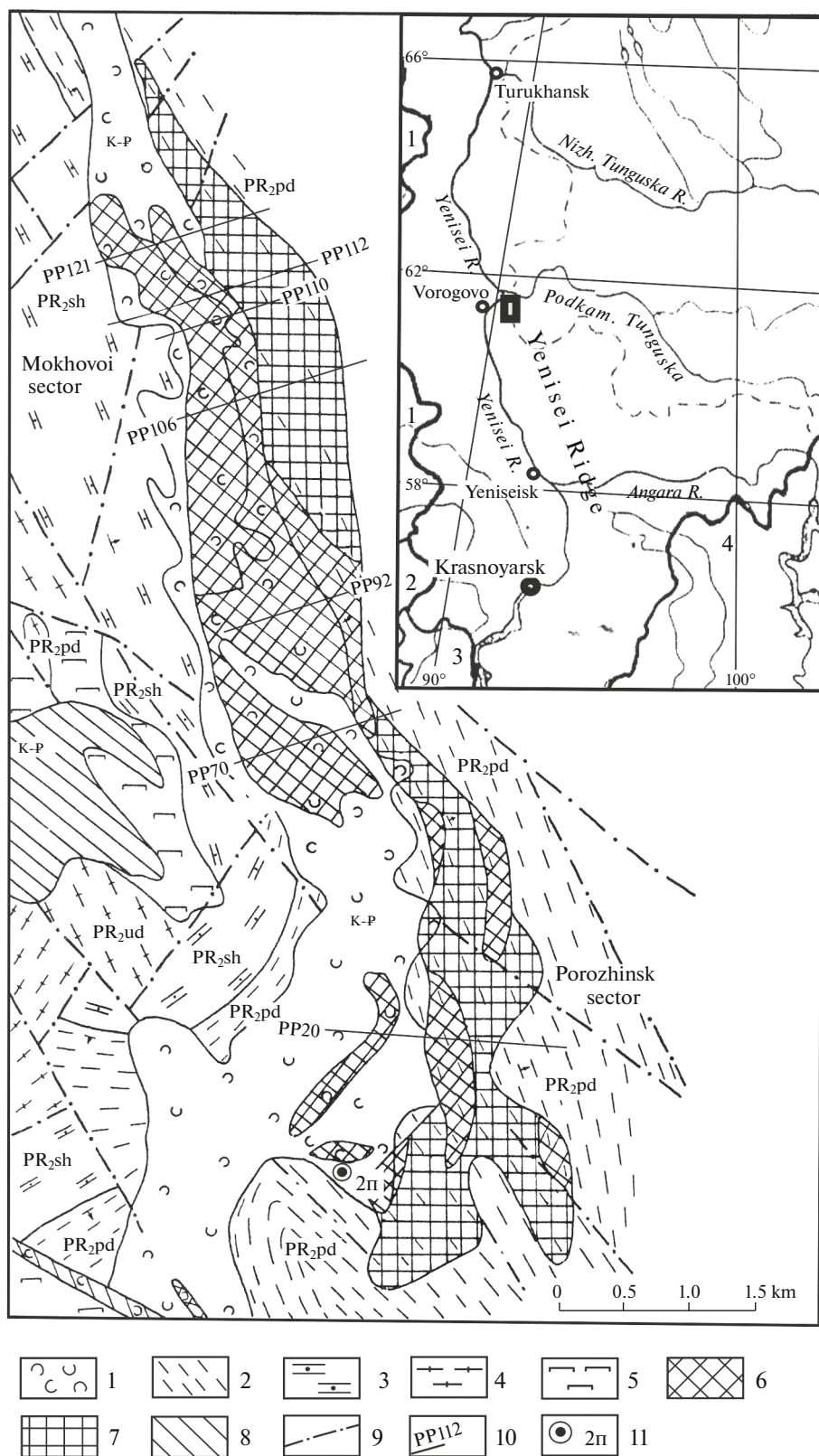


**Fig. 1.** Schematic geological map of the Mokhovoi and Porozhinsk ore sectors (modified after (Gorshkov, 1994). (1) Rocks of the weathering crust; (2) volcanosedimentary rocks of the Pod'mensk Formation; (3) carbonate rocks of the Sukhorechensk Formation; (4) schists of the Uderei Formation; (5) ultramafic rocks; (6–8) ore fields: (6) manganese oxide, (7) manganese carbonates, (8) silicate and nickel ores in weathered ultramafics; (9) faults; (10) exploration profiles; (11) position of prospecting hole 2p. Inset shows the location of the Porozhinsk manganese deposit (black box, out of scale). Numerals in the inset: (1) Tomsk district, (2) Kemerovo district, (3) Khakassia Republic, (4) Irkutsk district.

tion of reserves and substations of technical-economic cut-off grade (Porozhinsk prospecting team, SC PGO "Krasnoyarskgeologiya" (1978–1990); MPC "Pluton" (1995–1998) were carried out to prepare this deposit for mining.

The results of prospecting works and studies at the Porozhinsk deposit have been reported in unpublished reports and several publications (Mkrtych'yan et al., 1980; Golovko and Nasedkina, 1982; Golovko et al., 1982; Ustalov, 1982; Mstislavsky and Potkonen, 1990; Tsykin and Sviridov, 1993, 2012; Gorshkov, 1994; Kuleshov, 2018; Kuleshov et al., 2021a, and others). For this reason, the general characteristics of the deposit as well as geological position of rocks and ores developed here are briefly reviewed.

The Porozhinsk deposit is confined to the Porozhinsk syncline, which complicates the structure of the Mikheev depression in the Vorogovka trough. The oldest rocks in the deposit area are referred to the Lower Proterozoic and divided into three formations: Porozhinsk (two-mica garnet plagiogneisses, garnet amphibolites, calciphyres, and quartzites), Karpinsky Ridge (gneisses, quartzites, quartz–garnet–two-mica schists, marbles, and amphibolites), and Pechenga (crystalline schists, quartzites, and marbles) formations (Tsykin and Sviridov, 2012). They are unconformably overlain by rocks ascribed to the Lower–Middle Riphean Sukhopit Group made up of crystalline schists of diverse composition, quartzites, and marbles. All these rocks compose the structural basement of the Vorogovka trough and easterly areas of the Chapa–Teya trough, northern Yenisei Ridge, which are made up of Late Neoproterozoic complexes.

Within the Vorogovka trough, the upper parts of the Neoproterozoic section consist of the Vorogovka Group and overlying carbonate sequence. The Vorogovka Group is subdivided into the Severorechensk, Mutninsk, and Sukhorechensk formations, made up of variable proportions of terrigenous and carbonate rocks (Kirichenko, 1965; Sovetov and Blagovidov, 1996; Khomentovsky, 2015; Vishnevskaya et al., 2017; Kuznetsov et al., 2017). Their stratigraphic counterparts in the southwestern Chapa–Teya trough are the Chingasan Group subdivided into the Lopatin, Kar'er (Vandadak), and Chivida formations consisting mainly of terrigenous clastic and clayey rocks (Semikhatov, 1962; Khomentovsky et al., 1972; Nozhkin et al., 2007; Khomentovsky, 2015, Shatsillo et al., 2015; Kuznetsov et al., 2018; Priyatkina et al., 2016). The Late Neoproterozoic rocks developed in the northeastern parts of the Chapa–Teya trough are referred to the Chapa Group, which occupies the higher stratigraphic position relative to the Chingasan Group (Semikhatov, 1962, Khomentovsky, 2015, Priyatkina et al., 2016). The Chapa Group is usually subdivided into the Suvorovsk Formation (consisting of conglomerates that are locally developed and likely

filling the erosion pockets), essentially carbonate Pod'emsk Formation, and overlying Nemchan Formation consisting of red-colored terrigenous rocks (Sovetov, 1977; Sovetov and Blagovidov, 2004; Khomentovsky, 2015). By analogy with the generally accepted summary section of the Chapa–Teya trough, the upper units (mainly carbonates) of the Neoproterozoic sequence in the Vorogovka trough are also distinguished as the Pod'emsk Formation. As in the Chapa–Teya trough, the Neoproterozoic rocks in the Vorogovka trough are overlain by the Lower Cambrian Lebyazhino Formation (Ustalov, 1982; Khomentovsky, 2015; Priyatkina et al., 2016; Vishnevskaya et al., 2017; Kuznetsov et al., 2017).

In the Vorogovka trough, including the Porozhinsk deposit (central part of the Vorogovka trough), the carbonate rocks ascribed to the Pod'emsk Formation are manganese-bearing. The carbonate sequence is subdivided into the lower and upper subformations. The lower subformation is well persistent in composition and thickness. It is mainly composed of dolomites intercalated with mudstones and limestones near the roof. Total thickness of the formation is 360–400 m. The rocks ascribed to the Upper Pod'emsk subformation at the Porozhinsk deposit have the elevated manganese content and contain (up to the predominance) tuffaceous and tuffaceous–siliceous rocks (Ustalov, 1982; Tsykin and Sviridov, 1993, 2012). This sequence is subdivided into six units (Mn-bearing volcano-genic–terrigenous, tuffaceous silicitic, silty–tuffaceous silty, carbonate–tuffaceous–terrigenous, silty–sandy units with lenses of stromatolitic limestones, and calcareous–sandy unit) with the variable inner structure (Tsykin and Sviridov, 1993, 2012). The main productive Mn-bearing unit is the first (lower) unit, which includes the stratiform rhodochrosite tuffaceous siltstones, psammitic tuffs, and tuffites with the average manganese content 8–10%, sometimes higher (Golovko et al., 1982). The tuffs contain numerous dolomite–rhodochrosite and rhodochrosite nodules and fragments of the same composition, which occasionally reach up to 20–60 vol % of clastic material and are grouped into stratiform ore layers.

Slightly elevated manganese content was also found in the upper units of the subformation, which contain limestone horizons; separate limestone intercalations bear admixture of organic matter in form of bitumens and coaly–graphitic enclaves. Thickness of the sequence ascribed to the upper Pod'emsk subformation varies from 800 to 2100 m over the deposit.

Rocks of the upper Pod'emsk subformation are conformably overlain by the sequence of alternating inequigranular mudstones, siltstones, and sandstones, which is usually (Khomentovsky, 2015) correlated with the Nemchan Formation of the Chapa Group in the Chapa–Teya trough. This group is ascribed to the Lower Vendian (Pokrovsky et al., 2012) or upper parts

of the Upper Vendian (Ediacaran) (Priyatkina et al., 2016).

The Phanerozoic sequences in the deposit area are represented by the Lower Paleozoic, Mesozoic–Early Cenozoic rocks, and loose Quaternary deposits. The Lower Paleozoic includes the faunally characterized Lower Cambrian, mainly carbonate rocks of the Lebyazhino Formation. In the Vorogovka trough (as in the Chapa–Teya trough), this formation rests on the rocks of the upper part of the Nemchan Formation. In some other parts of the Yenisei Ridge (for instance, upper reaches of the Vorogovka River), it lies on the older rocks. The Lebyazhino Formation is dominated by the dolomites, with scarce siltstone, mudstone, and gypsum units (Ustalov, 1982; Tsykin and Sviridov, 1993, 2012).

The Mesozoic–Early Cenozoic rocks were formed in a continental setting and compose mainly areal and linear weathering crusts (Mkrtych'yan et al., 1980; Golovko and Nasedkina, 1982; Golovko et al., 1982; Ustalov, 1982; Mstislavsky and Potkonen, 1990; Tsykin and Sviridov, 1993, 2012; Gorshkov, 1994). In many cases, these rocks fill cavities in karst depressions developed in the carbonate rocks ascribed to the Pod'emsk Formation. There are also occasionally preserved Middle–Upper Jurassic, Lower Cretaceous, and Paleogene carbonaceous–terrigenous and terrigenous rocks, as well as their weathering products (Tsykin et al., 1987).

The Porozhinsk deposit combines seven conditionally outlined sectors (Kozhevsky, Mokhovoi, Porozhinsk, Tsentral'nyi, Khrebtovyi, Severnyi, and Mikheev–Mutninsk) (Gorshkov, 1994; Tsykin and Sviridov, 2012). The largest manganese reserves were found in the Mokhovoi and Porozhinsk sectors (Gorshkov, 1994).

Primary manganese and manganese-bearing rocks at the Porozhinsk deposit are confined to the sequence ascribed to the upper subformation of the Upper Vendian Pod'emsk Formation. These are carbonate rocks (manganese-bearing dolomites and others) with elevated manganese content (MnO 6% or higher). Secondary (supergene, superimposed) manganese ores are related to the Mesozoic–Early Cenozoic weathering crusts and are composed mainly of oxide ores, with subordinate (up to 3%) manganese carbonates.

The superimposed carbonate manganization is expressed in pseudomorphous metasomatic replacement of dolomite by rhodochrosite and manganocalcite, as well as formation of rhodochrosite veinlets and pockets. These processes are caused by the infiltration of Mn-rich groundwaters through fractured cavernous dolomites and by metasomatism of the latter with the formation of supergene rhodochrosite and manganocalcite (Tsykin et al., 1987; Golovko et al., 1982; Tsykin, 1984, 1992; Gorshkov, 1994; Tsykin and Sviridov, 2012).

Manganese ores in karst depressions compose a series of subparallel stratal and lenticular horizontal and inclined orebodies, which are complicated by local salients and saggings. These stratal and lenticular orebodies frequently contain barren “inclusions” (“windows”). The orebodies are conformable to units of clayey rocks of Mesozoic–Cenozoic areal and linear weathering crusts (Gorshkov, 1994; Tsykin and Sviridov, 2012).

The manganese rocks and ores of the Porozhinsk deposit were formed under different conditions for a long geological time, from Vendian to Cretaceous–Paleogene. According to the widespread point of view (Ustalov, 1982; Gorshkov, 1994; Tsykin and Sviridov, 1993, 2012, and others), manganese was initially accumulated as carbonates (manganese-bearing dolomite, rhodochrosite, manganocalcite, and manganosiderite), which are typical of the Upper Vendian section (upper Pod'emsk subformation). In the Cretaceous–Paleogene, karst deposits developed mainly after rocks ascribed to the upper Pod'emsk subformation, which served as manganese source for ores of the deposit. Manganese is mainly accumulated as oxides (psilomelane, pyrolusite, vernadite, rancieite, birnessite, and others) and manganite at depths more than 200 m). The formation of secondary (supergene) manganese carbonates (rhodochrosite, manganocalcite, kutnorhorite) is also widespread and repeatedly noted in the Mesozoic–Cenozoic (Golovko et al., 1982; Tsykin, 1984, 1992; Tsykin et al., 1987).

It should be noted that the bottom of the karst depressions is usually composed of dolomites ascribed to the lower Pod'emsk subformation (Fig. 2), which are frequently characterized by the elevated manganese content and likely could serve as a manganese source for orebodies in the karst depressions (Kuleshov et al., 2021a).

Thus, manganese carbonates and host rocks of the Porozhinsk deposit were formed under principally different conditions at different stages of formation: marine conditions in the Late Vendian and continental conditions (related to the formation of karst depressions) in the Late Mesozoic and Early Cenozoic. This could affect the isotope (strontium, carbon, and oxygen) systems of rocks and ores of the deposits.

## MATERIALS AND ANALYTICAL METHODS

### *Material*

The studied 16 samples, taken from collections of several geologists and geological organizations, comprises carbonate and oxide manganese ores and host dolomites. The material was mainly sampled from the core of prospecting and exploration holes drilled in the Porozhinsk and Mokhovoi sectors, as well as from technological samples. The position of the studied samples is assigned to the prospecting holes (core: profile, hole number, and sampling depth), prospect-

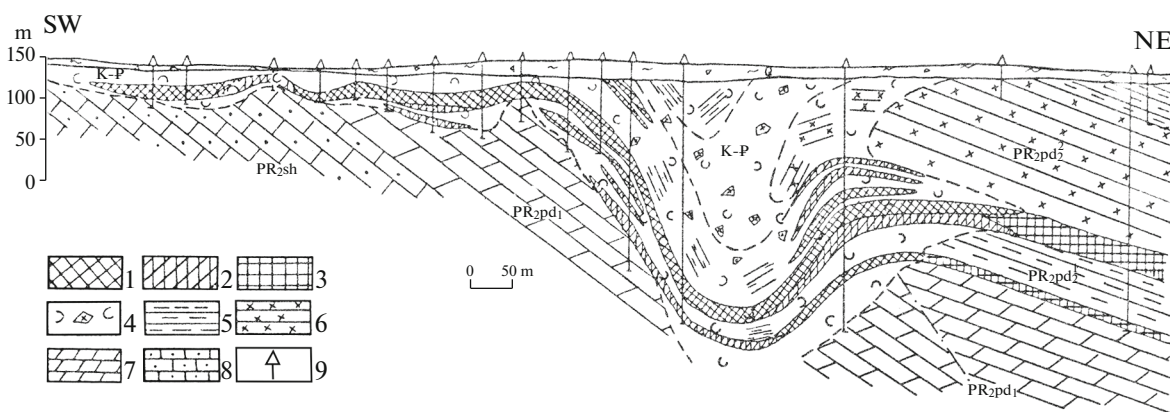


**Fig. 2.** Geological section along profile 112 of the Mokhovoi sector of the Porozhinsk deposit (Gorshkov, 1994). (1–3) ores: (1) oxide, (2) oxide–carbonate, (3) carbonate; (4) rubbly–clayey rocks (weathering crust); (5) siltstones, tuffaceous siltstones, tuffstones; (6) silicites and phthanites; (7) dolomites; (8) sandy limestones; (9) position of boreholes.

ing pits and trenches (prospecting profiles, stakes). We were unable to correlate stratigraphically the studied dolomites, but could estimate their relative position (within section) based on the depth of the studied samples.

#### Analytical Methods

The carbonate constituent (calcite, rhodochrosite, dolomite) for the Sr isotope analysis was extracted by dissolution in 1 N HCl. Prior to measurements, the samples were subsequently washed in 0.1 N HCl and in Milli-Q ultrapure water. The strontium isotope composition, rubidium and strontium contents were determined by the isotope dilution using mixed  $^{87}\text{Rb}$  and  $^{84}\text{Sr}$  spikes. The Sr and Rb isotope compositions were analyzed on a MAT-260 mass-spectrometer in the Laboratory of Isotope Geochemistry and Geochronology of the Geological Institute of RAS. The  $^{87}\text{Sr}/^{86}\text{Sr}$  ratio was determined with an accuracy of  $\pm 0.00008$ . Error in  $^{87}\text{Rb}/^{86}\text{Sr}$  determination was no more than 1.5% and was controlled by the measurement of ISG standard using technique (Vinogradov and Chernyshev, 1987).

Carbonate samples and KH-2, C-O-1, and NBS-19 standards for mass-spectrometric measurements were decomposed in orthophosphoric acid ( $\text{H}_3\text{PO}_4$ ) at  $50^\circ\text{C}$ . The carbon and oxygen isotope compositions were analyzed using a Thermoelectron system including Delta V Advantage mass-spectrometer coupled with a Gas-Bench-II unit. The  $\delta^{13}\text{C}$  values are given in per mille (‰) relative to the V-PDB standard;  $\delta^{18}\text{O}$  values, in per mille relative to the V-SMOW standard. The reproducibilities of  $\delta^{18}\text{O}$  and  $\delta^{13}\text{C}$  determinations are within  $\pm 0.2\text{‰}$  and  $\pm 0.1\text{‰}$ , respectively.

#### ANALYTICAL DATA AND DISCUSSION

The obtained chemical and isotope compositions ( $^{87}\text{Sr}/^{86}\text{Sr}$ ,  $\delta^{18}\text{O}$ ,  $\delta^{13}\text{C}$ ) of the studied rocks and ores are presented in Tables 1 and 2. Noteworthy is the wide range of Sr isotope ratio ( $^{87}\text{Sr}/^{86}\text{Sr}$  from 0.70822 to 0.70924), as well as carbon ( $\delta^{13}\text{C}$ :  $-14.6\text{‰}$ ... $2.0\text{‰}$ , PDB) and oxygen ( $\delta^{18}\text{O}$  =  $9.4\text{‰}$ ... $28.3\text{‰}$ , SMOW) isotope compositions. This indicates different conditions of formation (and, likely, transformation) and different sources of the studied rocks.

*Carbon and oxygen isotope composition.* The obtained carbon and oxygen isotope data are shown in Fig. 3. It is seen that the isotope characteristics of the studied rocks correspond to diverse genetic types of carbonates. The highest ( $\delta^{13}\text{C} \approx -1\text{‰}$ ... $2\text{‰}$ )  $\delta^{13}\text{C}$  and  $\delta^{18}\text{O}$  values correspond to dolomites formed in marine environment (fields A and B). As expected, the manganese carbonates have the lightest carbon isotope composition ( $\delta^{13}\text{C} = -14.6\text{‰}$ ... $-9.5\text{‰}$ ). This indicates that they were formed with the assistance of oxidized organic carbon both in initial sediments of the early diagenetic zone (field C) and under exogenic (karst depressions) conditions (Fig. 3, field D). All  $\delta^{13}\text{C}$  and  $\delta^{18}\text{O}$  data on carbonates of the Porozhinsk deposit are reported in (Kuleshov, 2018; Kuleshov et al., 2021a).

The  $\delta^{18}\text{O}$  values in dolomites show wide variations ( $22.3\text{‰}$ ... $28.5\text{‰}$ ), whereas their carbon isotope composition, in general, remains sufficiently stable ( $\delta^{13}\text{C} \approx -1\text{‰}$ ... $2\text{‰}$ ) and corresponds to those of marine carbonates (Degens, 1967, 1971].

In particular, the highest  $\delta^{18}\text{O}$  ( $27.6\text{‰}$ ... $28.5\text{‰}$ ) are typical of dolomites taken from the deepest (depths 200 m and lower) horizons ascribed to the lower Pod’emsk subformation. In Fig. 3, data points corresponding to these values occupy field A. At the same time, the majority of dolomites are characterized by the light oxygen isotope composition ( $\delta^{18}\text{O}$   $22\text{‰}$ ... $26\text{‰}$ )

**Table 1.** Isotope composition ( $\delta^{13}\text{C}$ ,  $\delta^{18}\text{O}$ ),  $^{87}\text{Sr}/^{86}\text{Sr}$ ,  $^{87}\text{Rb}/^{86}\text{Sr}$ , Mn/Sr and MnO content (%) in the carbonate rocks and ores of the Pod'emska Formation of the Porozhinsk manganese deposit (Yenisei Ridge, Krasnoyarsk region)

An. no.	Sample no.	Sample characteristics	$^{87}\text{Sr}/^{86}\text{Sr}$	$^{87}\text{Rb}/^{86}\text{Sr}$	Initial $^{87}\text{Sr}/^{86}\text{Sr}$ at 550 Ma	Sr, ppm	Rb, ppm	$\delta^{13}\text{C}$ , ‰ PDB	$\delta^{18}\text{O}$ , ‰ SMOW	MnO, %	Mn/Sr	Ce/Ce* <sub>xx</sub>	Mg/Ca	$\text{SiO}_2$ , %
7325	2p-2/45.0	<i>Porozhinsk sector</i> , karst depression, hole group; hole, 2p-2, depth 45.0 m. Manganese dolomite.	0.70851	0.06	0.70800	40.0	0.82	1.8	24.3	1.07	207.5	1.94	0.554	0.25
7319	2p-3/50.0	The same, hole 2p-3, depth 50.0 m. Carbonate manganese ore.	0.70924	0.15 <sup>x</sup>	0.70807	32.4	1.74	-14.6	21.3	28.20	6697.5	1.03	0.263	13.0
7332	2p-4/5.4	The same, hole 2p-4, depth 5.4 m. Carbonate manganese ore, sandy.	0.70862	0.05	0.70823	28.6	0.49	-9.5	19.4	36.60	9853.2	0.98	0.375	18.7
7334	2p-5/34.3-35.3	The same, hole 2p-5, depth 34.3–35.3 m. Manganese dolomite.	0.70855	0.0005	0.70854	52.1	0.17	1.0	27.7	6.10	959.7	–	0.507	1.57
7425	019/278.2	The same; pr. 20, hole 19, depth 278.2 m. Dolomite.	0.70826	0.020	0.70810	72.9	0.24	0.6	28.5	0.51	57.6	1.02	0.576	3.47
7428	021/200.0	The same, pr. 20, hole 21, depth 200.0 m. Dolomite.	0.70854	0.007	0.70848	46.4	0.12	0.1	27.6	0.16	84.1	1.07	0.572	1.88
7322	110/30.50-2	<i>Mokhovoi area</i> , PP* 110, sample ST** 30.50-2. Manganese dolomite.	0.70858	0.22 <sup>x</sup>	0.70686	28.3	2.15	1.7	23.1	1.06	289.8	–	0.558	0.86
7323	110/30.50-3	The same area, SL 110, sample ST 30.50-3. Manganese dolomite.	0.70839	0.021	0.70822	30.6	0.23	1.5	25.7	1.57	395.4	–	0.537	3.0
7324	110/30.50-4	The same, PP 110, sample ST 30.50-4. Dolomite.	0.70859	0.019	0.70844	25.7	0.17	1.9	22.5	0.40	120.6	–	0.537	0.22
7329	B-11012/30.19	The same, PP 110, sample B-11012, ST 30.19. Dolomite.	0.70864	0.051	0.70824	42.1	0.74	2.0	22.3	0.83	152.0	–	0.535	0.17
7330	B-11012/30.33	The same, PP 110, sample B-11012, 30.33. Manganese dolomite.	0.70900	0.008	0.70894	33.3	0.09	2.0	22.5	2.70	624.6	0.99	0.516	0.17
7331	B-11012/30.50	The same, PP 110, sample B-11012, ST 30.50. Dolomite.	0.70847	0.005	0.70843	36.9	0.061	1.8	22.9	0.35	73.2	–	0.565	0.09
7336	SL92/TP-1-4	The same, SL92, sample TP*** 1-4. Dolomite.	0.70840	0.027	0.70817	37.3	0.35	-1.9	25.3	0.15	32.2	2.34	0.554	0.76
7430	10614/190.9	The same, pr. 106, Hole 14, depth 190.9 m. Oxide-carbonate ore; scarce quartz grains.	0.70822	0.029	0.70800	239.4	2.4	-9.8	26.4	15.38	494.6	1.0	0.249	46.11
7432	12105/301.4	The same, pr. 121, hole, 5, depth 301.4 m. Dolomite.	0.70825	0.006	0.70820	41.2	0.08	1.2	28.3	0.31	58.3	1.02	0.580	4.75
7436	7001/249.0	The same; pr. 70, hole 1, depth 249.0 m. Dolomite.	0.70827	0.007	0.70821	63.8	0.15	-0.4	27.7	0.43	52.4	1.07	0.386	1.09

(\*) high  $^{87}\text{Rb}/^{86}\text{Sr}$  ratios are likely caused by later contamination of samples; (\*\*) see (Kuleshov et al., 2021).



**Table 2.** Chemical composition of major components (wt %) in carbonate rocks of the deposits of the Yenisei Ridge

Components	Sample no.															
	7319	7322	7323	7324	7325	7329	7330	7331	7332	7334	7336	7425	7428	7430	7432	7436
SiO <sub>2</sub>	13.0	0.86	3.0	0.22	0.25	0.17	0.17	0.09	18.7	1.57	0.76	3.47	1.88	46.11	4.75	1.09
TiO <sub>2</sub>	0.33	0.13	0.028	0.006	0.011	0.009	0.007	0.005	0.19	0.032	0.006	0.04	0.01	0.25	0.02	<DL
Al <sub>2</sub> O <sub>3</sub>	8.7	0.43	0.95	0.13	0.14	0.13	0.11	0.079	4.2	0.79	0.30	1.42	0.71	6.08	0.94	0.48
Fe <sub>2</sub> O <sub>3</sub> <sup>tot</sup>	13.8	0.41	0.47	0.14	0.47	0.23	0.63	0.16	6.2	1.21	0.12	1.36	0.67	3.66	1.10	1.14
MnO <sup>tot</sup>	28.2	1.06	1.57	0.40	1.07	0.87	2.70	0.35	36.6	6.1	0.15	0.51	0.16	15.38	0.31	0.43
MgO	1.40	20.4	19.6	20.6	20.5	20.4	19.5	21.3	1.96	17.7	20.9	19.20	20.29	2.95	19.33	15.85
CaO	4.5	30.9	30.8	32.4	31.3	32.2	31.9	31.8	4.2	29.5	31.9	28.19	29.98	10.00	28.19	34.65
Na <sub>2</sub> O	0.12	0.042	0.954	0.051	0.045	0.046	0.048	0.038	0.040	0.046	0.038	0.09	0.08	0.60	0.07	0.05
K <sub>2</sub> O	0.8	<0.03	<0.03	<0.03	<0.03	<0.03	<0.03	<0.03	0.54	<0.03	<0.03	0.31	0.18	0.81	0.17	0.13
P <sub>2</sub> O <sub>5</sub>	0.91	0.028	0.033	0.038	0.042	0.029	0.040	0.022	0.58	0.039	0.019	0.06	0.05	0.31	0.08	0.29
S	0.24	0.01	0.06	<0.01	<0.01	<0.01	<0.01	<0.01	0.84	0.01	0.01	0.024	0.012	<0.01	<0.01	<0.01
L.O.I.	27.47	45.33	44.52	45.66	45.5	45.71	44.78	45.84	24.66	42.93	45.39	45.28	45.94	13.50	44.97	45.83
Total	99.8	99.5	101.98	99.6	99.3	99.7	99.8	99.7	99.9	100.0	99.6	99.95	99.97	99.71	99.98	99.96

(<DL) below the detection limit.

and occupy the conditional field B. Close  $\delta^{18}\text{O}$  value was also found in manganese carbonate (rhodochrosite) from sequences ascribed to the lower Pod''emsk subformation ( $\delta^{18}\text{O} = 26.4\text{‰}$ , Table 1). This manganese carbonate was likely formed in the early diagenetic zone, when exchange between bottom and mud waters still continued in sedimentation basin (Fig. 3, field C) (Kuleshov et al., 2021a).

Thus, we may suggest that dolomites ascribed at the Porozhinsk deposit (Mikheev Depression of the Vorogovka trough) to the Pod''emsk Formation were formed under different isotope-geochemical conditions likely caused by diverse paleofacies environments, formation temperatures, and oxygen isotope composition of seawater, which could vary in over area) and time.

It should be noted that wide variations of the oxygen isotope composition in the Late Neoproterozoic dolomites, in general, are typical of sequences in areas adjacent to the Vorogovka trough and many Siberian regions. For instance, the  $\delta^{18}\text{O}$  values are 23.1...25.6‰ in dolomites and 21.0...22.1‰ in limestones of the Pod''emsk Formation from the Chapa River section (Pokrovsky et al., 2012). Wide isotope variations ( $\delta^{18}\text{O} = 25.3\text{‰}...28.1\text{‰}$ ) are also typical of dolomites from the Ediacaran Taseev Formation of the southern Yenisei Ridge (Kochnev et al., 2020). Wide oxygen isotope variations were found in dolomites of the transitional Vendian (Ediacaran) to Cambrian (Dikimda Formation) sequences on the western slope of the Aldan shield (Olekma River). The  $\delta^{18}\text{O}$  values in these rocks also widely vary from 24.9 to 28.3‰ (Pokrovsky et al., 2020).

Wide variations of  $\delta^{18}\text{O}$  values in the Late Neoproterozoic dolomites were also found in other regions of Siberia. In particular, the diverse lithological types (clayey, calcareous, anhydritic, saliferous, and others) of Vendian dolomites from central parts of the Siberian Platform are also characterized by the sufficiently wide range of these values. For instance, these values in the Uspun Formation are 24.4...25.4‰ (Western Botuobinskaya-362-0 hole), 25.6...27.3‰ (Sokhsolokhszkaya-706 hole); those of the Byuk Formation of the Tira unit are 27.6...29.6‰ (Aikhal'skaya-707 hole), 24.7...30.9‰ (Western Botuobinskaya-362-0 hole), 30.3...31.3 (Onkuchakhskaya-286-1 hole), 28.5...31.8‰ (Sokhsolokhszkaya-706), 28.6...32.0‰ (Khanninskaya-322-0 hole), 29.1...30.2‰ (Sheinskaya-471 hole); and 25.7...28.7‰ in the Kharystan Formation of the Nepa horizon (Khaninskaya-322-0 hole). In the Parshin Formation of the Nepa horizon, the  $\delta^{18}\text{O}$  values in dolomites are slightly lower and account for 24.6...25.2‰ (Chaikinskaya-279 hole) and 21.6...26.2‰ (Chaikinskaya-367 hole). At the same time, these values in rocks of the Ynakh Formation of the Nepa horizon have the higher values of 29.0...30.8‰ (Sheinskaya-471 hole) (Kochnev et al., 2018). As will be shown below, similarly wide oxygen isotope variations are also typical of Ediacaran carbonates worldwide.

It should be noted that the interpretation of wide variations of  $\delta^{18}\text{O}$  mentioned in the cited works did not receive significant attention. However, these data bear important information on formation (sedimentation) conditions of carbonates, because reflect a change of both temperature conditions and oxygen isotope com-

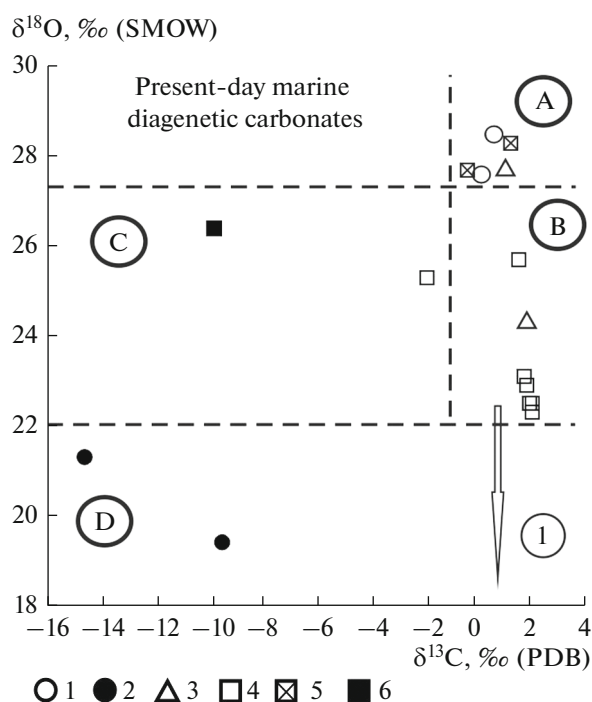


**Fig. 3.**  $\delta^{13}\text{C}$  and  $\delta^{18}\text{O}$  in rocks and ores of the Porozhinsk manganese deposit. (A) field of the present-day sedimentary marine carbonates, (B) inferred field of Late Precambrian–Early Paleozoic sedimentary marine carbonates of the Vorogovka trough, (C) inferred field of Late Precambrian–Early Paleozoic diagenetic marine carbonates of the Vorogovka trough; (D) field of carbonates from supergene zone. Arrow 1 shows the trend of  $\delta^{18}\text{O}$  under supergene secondary processes. (1–3) Porozhinsk sector: (1) dolomites of the lower Pod’emsk subformation, (2) manganese carbonates (ore) of the karst depression, (3) dolomites from the karst depression (Upper Pod’emsk (?) subformation), (4–6) Mokhovoi sector: (4) dolomites from prospecting trenches (Upper Pod’emsk (?) subformation), (5) dolomite from drill core (lower Pod’emsk subformation), (6) manganese carbonate.

position of waters in sedimentation basin (for instance,  $\delta^{18}\text{O}$  variations within 10‰ could indicate temperature changes up to 40°–50° or variations of seawater  $\delta^{18}\text{O}$ , or combined effect of these factors (Friedman, O’Neil, 1977)).

Sharp shifts of  $\delta^{18}\text{O}$  values are frequently observed even within single section. For instance, sharp shifts (by 3–4‰) observed at the contact of limestones and dolomites in the Vendian reference sequence of the Urin Rise (northeastern Paton trough) (Pokrovsky and Bujakaite, 2015, p. 165) are thought to be related to the “... significant change of sedimentation conditions and hiatus”.

Sufficiently sharp shifts of  $\delta^{18}\text{O}$  (up to 8–10‰) on transition from dolomites to limestones are also typical of different sequences of the transitional Vendian–Cambrian sequences in the Tsagaan Oloom and Bayan Gol Formations of the Dzabkhan basin (West-

ern Mongolia): in sections along the Bayan-Gol Creek, Khevte-Tsakhir-Nuru ridge, and Tsagaan-Gol Creek (Kuleshov and Zhegallo, 1997). This was likely caused by not only secondary alterations, but also by primary reasons, in particular, by a change of sedimentation conditions (temperature factor and desalination of paleobasin).

Thus, according to our observations (rocks of the Porozhinsk deposit) and data presented in the cited works, Neoproterozoic dolomites were likely formed in marine basins under different sedimentation conditions, which resulted in the formation of both isotopically heavy (27...30‰) and isotopically light (22–24...27‰) rocks; the latter were likely precipitated from seawaters with lighter oxygen composition relative to modern ocean and at higher temperatures (Kuleshov et al., 2021a).

At the same time, some dolomites with the lightest oxygen isotope composition ( $\delta^{18}\text{O}$  22‰ and lesser) could experience secondary alterations by the isotopically light percolating fluids (probably, meteoric) owing to the oxygen isotope exchange between water and dolomites, which led to enrichment of the latter in light  $^{16}\text{O}$  (Fig. 3, arrow 1). In this case, the percolating solutions should not contain low- $\delta^{13}\text{C}$  dissolved carbon dioxide.

The enrichment of percolating solutions in the isotopically light carbon dioxide  $\text{CO}_2$  formed by the oxidation of organic carbon would result in the formation of carbonates with the lowest  $\delta^{13}\text{C}$  and  $\delta^{18}\text{O}$  values (Fig. 3, field D), as during the formation of manganese carbonates in the karst depressions and secondary carbonatization (fine dissemination and cross-cutting veinlets) (Kuleshov et al., 2021).

**Strontium isotope composition.** The obtained Sr isotope data on the ore-bearing and barren carbonates of the Porozhinsk deposit are presented in Table 1. If the ore-bearing and barren carbonates of the studied deposit were formed at different conditions, as follows from the oxygen isotope data presented in Table 1 and previous work (Kuleshov et al., 2021), the studied rocks should significantly differ in the Sr isotope composition. Indeed,  $^{87}\text{Sr}/^{86}\text{Sr}$  values in them show sufficiently wide variations from 0.70825 to 0.70924. Thereby, the lowest Sr values (0.70825–0.70827) are typical of dolomites taken from drill core at the deepest horizons of the lower Pod’emsk subformation (250–300 m). The highest (0.70862–0.70924) values are observed in manganese carbonates from karst depression, while  $^{87}\text{Sr}/^{86}\text{Sr}$  ratio in shallow dolomites (recovered by prospecting pits and holes in the karst depression) occupies an intermediate position (0.70839–0.70864) (Table 1). The  $^{87}\text{Sr}/^{86}\text{Sr}$  variations in the studied rocks could be caused by both secular variations of the Sr isotope composition in seawater and secondary processes leading to contamination



(influx in the Sr isotope system of rock) by the radiogenic  $^{87}\text{Sr}$ .

Before discussing the Sr isotope data, it is important to examine whether the obtained analytical data are representative, i.e., to estimate the preservation of initial Sr isotope composition in carbonates and the degree of secondary alteration of the studied rocks. The peculiarities of Sr isotope system in dolomites are, first of all, caused by extremely low Sr contents (25.7–72.7 ppm, Table 1). The Rb content is also low (0.061–0.82 ppm), although some dolomites have sufficiently high Rb concentrations (up to 1.74–2.40 ppm, Table 1). However, the absence of trend in the  $^{87}\text{Rb}/^{86}\text{Sr}$ – $^{87}\text{Sr}/^{86}\text{Sr}$  diagram (see below) argues in support of contamination by the silicate component. In this relation, we suggest that samples were enriched in Rb at late stages. Therefore, the correction of Sr isotope ratios for age is not introduced, but shown in the table for illustration.

The degree of carbonate transformations is usually estimated using the Mn/Sr ratio, which is  $<10$  in the least altered dolomites (Kaufman et al., 1996; Podkovyrov et al., 1998; Semikhatov et al., 2004, 2009; Khabarov and Izokh, 2014; Kuznetsov et al., 2014). In the studied dolomites ascribed to the Pod’emsk Formation at the Porozhinsk deposit, the Mn/Sr ratio exceeds the indicated value by 3–5 to 900 times (Table 1). This testifies that the Mn/Sr ratio in carbonates from the Mn-bearing sedimentation basins cannot be used as the criterion of carbonate alteration. This is likely caused by the fact that the Mn-bearing sedimentation basins initially contained the elevated Mn concentrations (owing to the continental runoff or Mn influx with hydrothermal vents). Sediments in such basins, including carbonates, have the high Mn contents, which significantly exceed the Clarke value for this element.

An insignificant degree of transformation of the studied dolomites in the Porozhinsk deposit also follows from the oxygen isotope composition. The  $\delta^{18}\text{O}$  values in the studied dolomites, in general, are high and account for 22...28‰. Thereby,  $\delta^{13}\text{C}$  shows no correlation with  $\delta^{18}\text{O}$ , which could also serve as evidence for insignificant postsedimentary alterations, according to the existing concepts (Kaufman and Knoll, 1995; Podkovyrov et al., 1998; Semikhatov et al., 2004; Pokrovsky et al., 2012, 2020; Kochnev et al., 2018, 2020).

At the same time, the studied dolomites show peculiar chemical features, which indicate specifics of their formation. For instance,  $\delta^{18}\text{O}$  negatively correlates with  $^{87}\text{Sr}/^{86}\text{Sr}$  (Fig. 4a): carbonates with the high Sr isotope ratio have the lighter oxygen isotope composition (lowest  $\delta^{18}\text{O}$ ). Thereby, the lowest  $^{87}\text{Sr}/^{86}\text{Sr}$  and the highest  $\delta^{18}\text{O}$  values are typical of dolomites taken from the deepest horizons of the carbonate sequence ascribed to the lower Pod’emsk sub-

formation, while manganese carbonates from karst depression, in contrast, have the high  $^{87}\text{Sr}/^{86}\text{Sr}$  ratio and light oxygen isotope composition (lowest  $\delta^{18}\text{O}$  values). Dolomites recovered by prospecting trenches and holes in the karst depression occupy an intermediate position. They are characterized by the weakly expressed “trend” (or “dependence”) of  $\delta^{18}\text{O}$  versus  $^{87}\text{Sr}/^{86}\text{Sr}$  (Fig. 4a). In particular, dolomites with the heaviest oxygen isotope composition are characterized by the lowest Sr isotope composition, and vice versa. Such dependences are usually interpreted as mixing lines of two sources with opposite isotope and chemical characteristics or as “contamination” of primary matter (dolomites ascribed to the lower Pod’emsk subformation at the Porozhinsk deposit) by the superimposed processes, in particular, the transformation of initial dolomites by the surface meteoric (atmospheric) waters, which have the light oxygen isotope composition (low  $\delta^{18}\text{O}$ ) and are enriched in the radiogenic Sr (crustal contamination).

If an increase of  $^{87}\text{Sr}/^{86}\text{Sr}$  was caused by postsedimentary alterations under subsurface conditions, the dolomites would show a lighter carbon isotope composition (decrease of  $\delta^{13}\text{C}$ ) and simultaneous increase of MnO, because meteoric waters in the considered deposits should be significantly enriched not only in manganese, but also in isotopically light carbon dioxide formed by the oxidation of organic carbon (as observed in manganese carbonates of the karst depression). However, this is not the case. At significant  $\delta^{18}\text{O}$  variations, the carbon isotope composition in dolomites remains relatively stable ( $\delta^{13}\text{C} \approx -1...2\text{‰}$ ) and corresponds, as mentioned above, to the marine sedimentary carbonates (Degens, 1967, 1971). Thereby, supergene manganese carbonates in karst depressions have a very light carbon isotope composition ( $\delta^{13}\text{C} = -14.6...-9.5\text{‰}$ , Fig. 3).

The available analytical data are insufficient to provide unambiguous interpretation of the relationship between  $^{87}\text{Sr}/^{86}\text{Sr}$  and MnO (Fig. 4b). It is possible that some shallow dolomites (upper parts of the lower Pod’emsk subformation or the upper Pod’emsk (?) subformation) could be enriched in manganese and radiogenic strontium owing to their reworking by surface (supergene) waters. On the other hand, the absence of correlation between  $^{87}\text{Sr}/^{86}\text{Sr}$  and Mn in Fig. 4b indirectly suggests that the modern Sr isotope systems in dolomites of the deposit do not depend on the Mn concentration, and hence, the Mn/Sr ratio cannot be applied in this case.

At the same time, the isotope ( $\delta^{13}\text{C}$  of dissolved carbonic acid and  $\delta^{18}\text{O}$  of water) and chemical (including  $^{87}\text{Sr}/^{86}\text{Sr}$  ratio) compositions of seawater could be evolved by the end of Neoproterozoic, which likely affected the composition of the studied dolomites, as observed in our case.

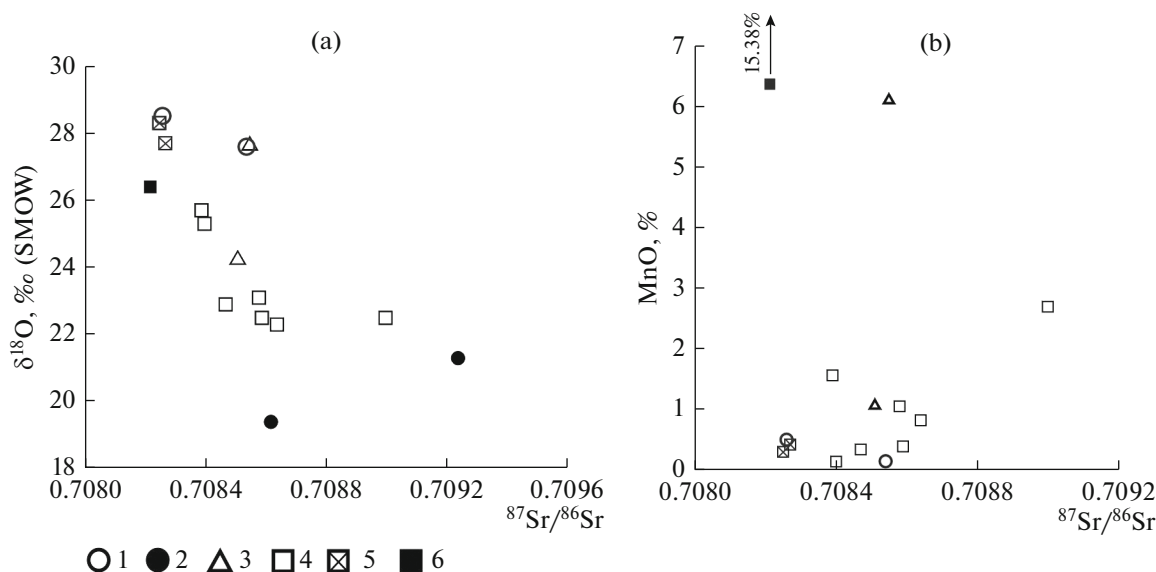


**Fig. 4.** Distribution of  $^{87}\text{Sr}/^{86}\text{Sr}$  versus  $\delta^{18}\text{O}$  (a) and MnO content (b) in rocks and ores of the Porozhinsk manganese deposit. (1–3) Porozhinsk sector: (1) dolomites of the lower Pod’emsk subformation, (2) manganese carbonates (ore) from karst depression, (3) dolomites from the karst depression (upper Pod’emsk (?) subformation); (4–6) Mokhovoi sector: (4) dolomites from prospecting trenches (upper Pod’emsk (?) subformation), (5) dolomite from drill cores (lower Pod’emsk subformation), (6) manganese carbonate (diagenetic).

We may also suggest that variations of  $^{87}\text{Sr}/^{86}\text{Sr}$  ratio in carbonate rocks of the Porozhinsk deposit could be related to a change of the continental runoff, i.e., influx of disintegrated rocks from the adjacent land, for instance, Lower Proterozoic metamorphic rocks (two-mica garnet plagiogneisses, garnet amphibolites, calciphyres, and quartzites of the Porozhinsk Formation; gneisses, quartzites, quartz–garnet–two-mica schists, marbles, and amphibolites of the Karpinsky Ridge Formation, and crystalline schists, calcites and marbles of the Pechenga Formation (Tsykin and Sviridov, 2012)). Figure 5 demonstrates distribution of the Sr isotope value versus lithochemical coefficient ( $\text{Al}_2\text{O}_3 + \text{TiO}_2$ ) in dolomites. Data points in this plot show no trends (composition points corresponding to dolomites ascribed at the Porozhinsk deposit to the lower Pod’emsk subformation are plotted in the left-hand part of the plot), which suggests an insignificant influence of the disintegrated rocks on the Sr isotope composition of dolomites.

As mentioned above, the insignificant transformation of primary carbonates may also be supported by the distribution of data points in the  $^{87}\text{Sr}/^{86}\text{Sr}$ – $^{87}\text{Rb}/^{87}\text{Sr}$  diagram in Fig. 6 (excluding two samples with supposedly disturbed Rb–Sr-system, Table 1). The obtained data in general, show unsystematic distribution (data points corresponding to dolomites of the inferred lower Pod’emsk subformation occupy the left-hand side of the plot with the lowest isotope ratios), which indicates that the primary Sr isotope system was not significantly disturbed and the obtained isotope data are representative.

The degree of alteration of initial carbonates can also be determined using variations of the Sr isotope ratio versus Rb, Sr, Rb/Sr, Mg/Ca, Si, Fe and some other components, as was made for carbonates of the Doushantuo Formation in South China (Sawaki et al., 2010). Figure 7 also shows these dependences for dolomites of the Porozhinsk deposit. The absence of clear correlation of  $^{87}\text{Sr}/^{86}\text{Sr}$  with Rb (Fig. 7a) and Sr (Fig. 7b), Mg/Ca ratio (Fig. 7c), and  $\text{SiO}_2$  (Fig. 7d) and  $\text{Fe}_3\text{O}_4$  (Fig. 7e), as well as the absence of negative correlation with  $\delta^{13}\text{C}$  values (Fig. 7f) indicate an insignificant degree of postsedimentary transformation of the dolomites.

Hence, if the transformation of initial carbonates was assisted by the surface water enriched in carbon dioxide with the light carbon isotope composition and caused an increase of  $^{87}\text{Sr}/^{86}\text{Sr}$  ratio, the rocks would demonstrate a decrease of  $\delta^{13}\text{C}$  values. However, Figure 7 shows an opposite tendency: an increase of  $\delta^{13}\text{C}$  values with increasing  $^{87}\text{Sr}/^{86}\text{Sr}$  ratio.

We believe that variations of Ce anomaly ( $\text{Ce}/\text{Ce}_{\text{NASC}}^*$ ) versus  $^{87}\text{Sr}/^{86}\text{Sr}$  ratio are important for understanding the geochemical features of these carbonates (Fig. 8). As expected, the highest Sr isotope values were found in the supergene manganese carbonates from karst depression, which is related to the contamination by the crustal (radiogenic) Sr isotope. Thereby, dolomites ascribed to the Pod’emsk Formation are characterized by wide variations of the Sr isotope ratio and Ce anomaly (relative to NASC). This could be caused by principally different isotope-geo-

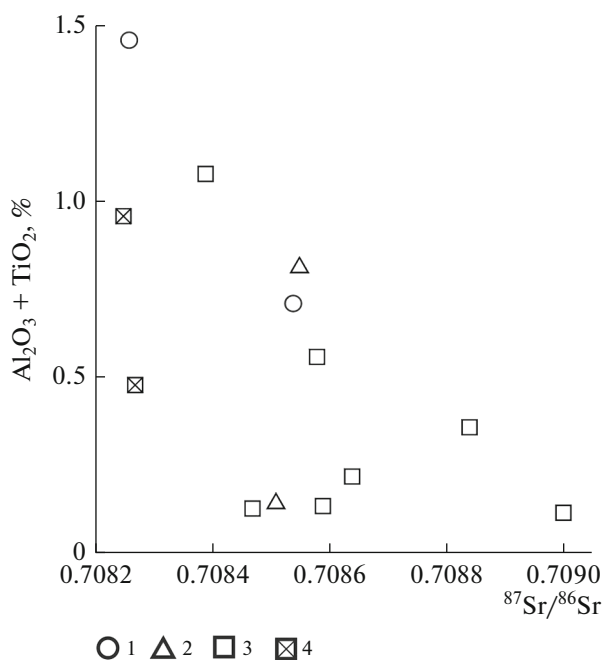


**Fig. 5.** Distribution of  $^{87}\text{Sr}/^{86}\text{Sr}$  and lithochemical coefficient ( $\text{Al}_2\text{O}_3 + \text{TiO}_2$ , %) in dolomites of the Porozhinsk deposit. (1, 2) Porozhinsk sector: (1) dolomites of the lower Pod'emska subformation, (2) dolomites from the karst depression (upper Pod'emska (?) subformation); (3, 4) Mokhovoi sector: (3) dolomites from prospecting trenches (upper Pod'emska (?) subformation), (4) dolomite from drill cores (lower Pod'emska subformation).

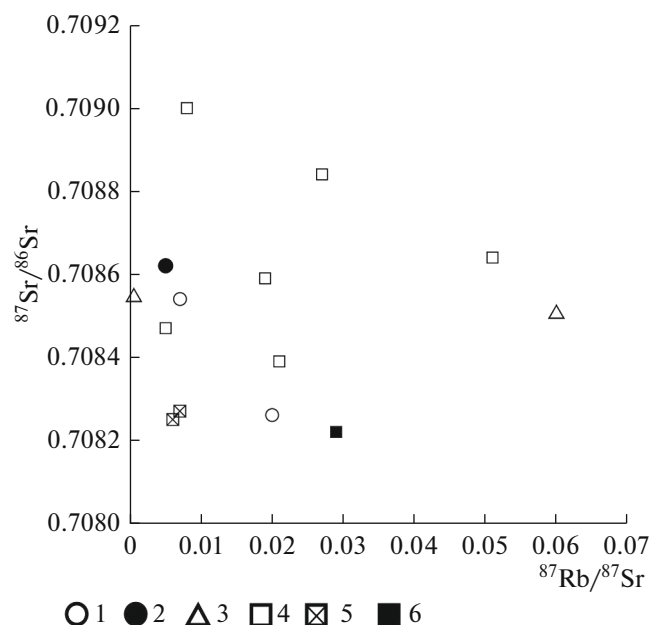


**Fig. 6.** Variations of  $^{87}\text{Sr}/^{86}\text{Sr}$  versus  $^{87}\text{Rb}/^{87}\text{Sr}$  in the dolomites of the Porozhinsk deposit. (1–3) Porozhinsk sector: (1) dolomites of the lower Pod'emska subformation, (2) manganese carbonates (ore) from karst depression, (3) dolomites from karst depression (upper Pod'emska (?) subformation); (4–6) Mokhovoi sector: (4) dolomites from prospecting trenches (upper Pod'emska (?) subformation), (5) dolomite from drill cores (lower Pod'emska subformation), (6) manganese carbonate (diagenetic).

chemical conditions of sedimentation in the Late Neoproterozoic marine basin (basins).

Thus, dolomites from deep horizons of the “lower Pod'emska” subformation of the Porozhinsk deposit have the heavier oxygen isotope composition ( $\delta^{18}\text{O} = 27\text{--}30\text{‰}$ ) and lowest  $\text{Ce}^*/\text{Ce}_{\text{NASC}}$  and  $^{87}\text{Sr}/^{86}\text{Sr}$  (field A, Figs. 4a, 8). In contrast, shallow dolomites (likely corresponding to the upper part of the “lower Pod'emska” and “upper Pod'emska” (?) subformations) are characterized by the lighter oxygen isotope composition ( $\delta^{18}\text{O} = 22\text{--}26\text{‰}$ ) and higher  $\text{Ce}^*/\text{Ce}_{\text{NASC}}$  and  $^{87}\text{Sr}/^{86}\text{Sr}$  (field “B”, Figs. 4a, 8). Hence, the isotope-geochemical conditions of their formation were different. The shallow dolomites were precipitated from seawater with a lighter oxygen isotope composition (likely also at elevated temperatures) and higher Sr isotope ratio; i.e., the isotope and chemical compositions of sedimentation basin have changed significantly.

A lack of negative Ce-anomalies in dolomites ascribed to the lower Pod'emska subformation indicates the absence or low concentration of free oxygen in seawater (basin or mud waters) during their precipitation. However, it is also possible that dolomites of this subformation were subjected to postsedimentary transformations, which caused the REE redistribution.

At the same time, a positive Ce anomaly in dolomites from the karst depression (“upper Pod'emska” subformation?) suggests that these dolomites were formed in anoxic conditions of shallow sedimentation basin with poor seawater circulation. Oxidized Ce could also be introduced into the paleobasin with the riverine colloids (Kuleshov et al., 2021b).

Thus, the considered above analytical data led us to conclusion that the observed tendencies in the distribution of  $\delta^{13}\text{C}$ ,  $\delta^{18}\text{O}$ ,  $\text{Ce}^*/\text{Ce}_{\text{NASC}}$ ,  $^{87}\text{Sr}/^{86}\text{Sr}$  and other parameters components (Rb, Sr, Mg/Ca,  $\text{SiO}_2$ ,  $\text{Fe}_3\text{O}_4$ ) in carbonate rocks of the Porozhinsk deposit could be caused mainly by the time-variable isotope and chemical properties (characteristics) of sedimentation environment (sea basin waters). The secondary (superimposed) processes, if occurred, did not affect significantly the  $^{87}\text{Sr}/^{86}\text{Sr}$ -ratio in the studied dolomites.

#### AGE AND POSSIBLE REASONS OF THE STRONTIUM ISOTOPE VARIATION IN DOLOMITES OF THE POD'EMSK FORMATION OF THE POROZHINSK DEPOSIT

As mentioned above, the Porozhinsk deposit is confined to the Porozhinsk syncline located within the

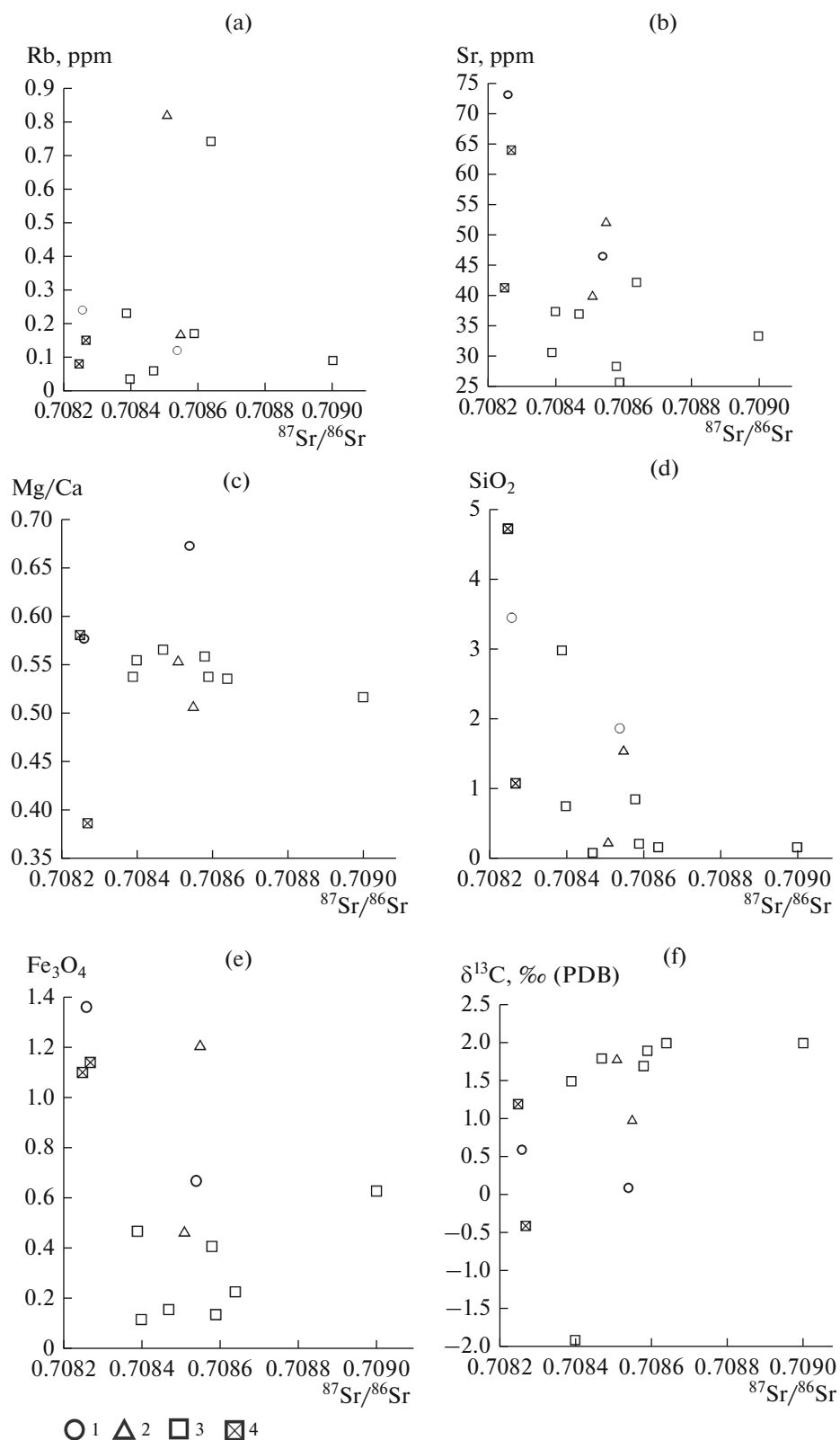


**Fig. 7.** Distribution of Rb (a), Sr (b), Mg/Ca (c),  $\text{SiO}_2$  (d),  $\text{Fe}_3\text{O}_4$  (e) and  $\delta^{13}\text{C}$  (f) versus  $^{87}\text{Sr}/^{86}\text{Sr}$  in the dolomites of the Porozhinsk deposit. (1–2) Porozhinsk sector: (1) dolomites of the lower Pod’emsk subformation, (2) manganese carbonates (ore) from karst depression, (3, 4) Mokhovo sector: (3) dolomites from prospecting trenches (upper Pod’emsk (?) subformation), (4) dolomite from drill cores (lower Pod’emsk subformation, horizons 200 m from the day surface and below).

Mikheev depression of the Vorogovka trough. There is no consensus concerning the age of rocks in this trough. The trough is filled with rocks of the Vorogovka Group (Upper Riphean (Ustalov, 1982; Khomentovsky, 2015) or Upper Vendian (Vishnevskaya et al., 2017; Kuznetsov et al., 2017)), Chapa Group including the Mn-bearing “Pod”emsk” Formation (Upper Riphean (Ustalov, 1982; Khomentovsky, 2015) or Upper Vendian (Priyatkina et al., 2016)), and Lower Cambrian Lebyazhino Formation.

According to the U–Pb-isotope dating of magmatic zircon from the volcanosedimentary matrix of diamictites widespread in middle reaches of the Vorogovka River, their age is  $696 \pm 4$  Ma (Rud’ko et al., 2020). Close age value ( $695 \pm 20$  Ma) was previously obtained on rocks of supradiamictite unit of the Chivida Formation (Pokrovsky et al., 2012).

Diamictites from middle reaches of the Vorogovka River are usually correlated with the Upper Riphean Chivida Formation of the Chingasan Group in the Chapa–Teya trough (Nozhkin et al., 2007), which is overlain by the Chapa Group, according to some researchers (Khomentovsky, 2015). If this is the case, counterparts of the Pod”emsk Formation of the Chapa Group in the Vorogovka trough of the Yenisei Ridge should be younger than diamictites from middle reaches of the Vorogovka River.

Unfortunately, the isotope dating of micas and zircon in pyroclastics from rocks ascribed to the upper Pod”emsk subformation at the Porozhinsk deposit has not been carried out yet. For this reason, the age of carbonate rocks of this stratigraphic unit can only be estimated using the strontium isotope chemostratigraphy (SIS), i.e., by the comparison of  $^{87}\text{Sr}/^{86}\text{Sr}$  ratio in the studied dolomites of the Porozhinsk deposit with those of coeval rocks from the adjacent portions of the Siberian Platform and its surrounding, as well as from distal sections in the Urals and China.

At present, the  $^{87}\text{Sr}/^{86}\text{Sr}$  ratio measured in carbonate rocks is widely applied in the intraregional, interregional, and global correlations of these rock sequences. The SIS method is an independent tool for the subdivision and correlation of “salient” carbonate sequences of different age, including the Upper Proterozoic sequence (Khabarov et al., 2002; Semikhatov et al., 2009; Kuznetsov et al., 2012, 2014; Vishnevskaya et al., 2017; Rud’ko et al., 2020, and others). This method is based on the analysis of long-term Sr isotope variations in paleoceans and paleoseas connected with them.

It is generally accepted that the  $^{87}\text{Sr}/^{86}\text{Sr}$  variations in the geological history of the World Ocean were caused by several global geodynamic factors, which led to the rearrangement in the Earth’s crust and mantle, and as a result, to changes in the balance of two main strontium fluxes: high  $^{87}\text{Sr}/^{86}\text{Sr}$  continental flux and low  $^{87}\text{Sr}/^{86}\text{Sr}$  mantle fluxes. The rapid mixing of waters bearing these strontium fluxes causes a rapid

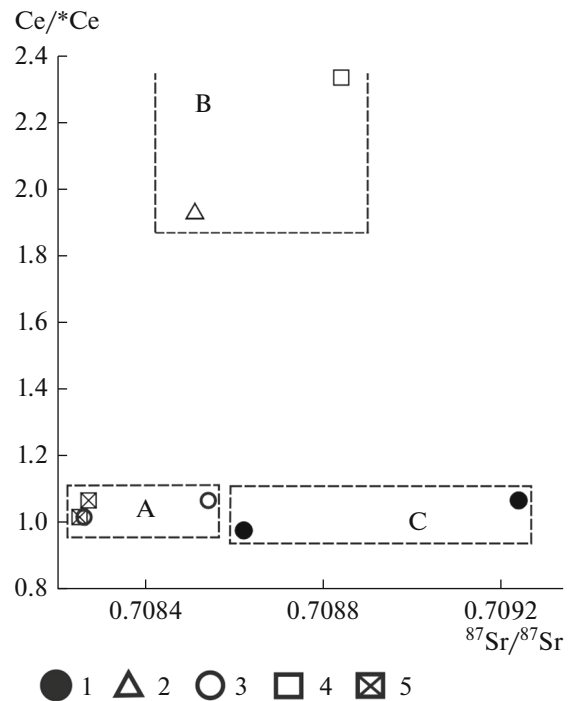


**Fig. 8.** Variations of cerium anomalies ( $\text{Ce}^*/\text{Ce}_{\text{NASC}}$ ) versus  $^{87}\text{Sr}/^{86}\text{Sr}$  ratio in the different types of carbonate matter. (1–3) Porozhinsk sector: (1) manganese carbonates (ore) from karst depression, (2) dolomites from karst depression, (3) dolomite from drill cores (lower Pod”emsk subformation, horizons 200 m and below the day surface); (4, 5) Mokhovoi sector: (4) dolomites from prospecting trenches, (5) dolomite from drill cores (lower Pod”emsk subformation, horizons 249 m from the day surface and below). (A) field of initial ratios in seawater during formation of dolomites of the lower Pod”emsk subformation, (B) inferred field of initial ratios in seawater during formation of dolomites of the lower Pod”emsk (likely also the upper Pod”emsk) subformations; (C) field of initial ratios in carbonic acid–water environment during formation of manganese carbonates from supergene zone.

(on a geological scale) global homogenization of the Sr isotope composition not only over the entire volume of the World Ocean (also by depth), but also in related marginal and inner seas (Kuznetsov et al., 2012, 2014).

The strontium isotope heterogeneity in oceans is determined by a long (a few million years) residence time of this element compared to the very rapid mixing (~a few thousand years). The high Sr content in oceanic waters compared to its content in river waters emptying into seas and oceans also serves as buffer of the strontium isotope ratio in the oceanic water (Faure, 1986).

In the geological evolution of lithosphere, the proportions of these strontium sources repeatedly changed. During the “piling” of continental blocks into composite continents and supercontinents, the marginal continental and intracontinental orogenic systems were formed. In the axial parts of these oro-

gens, the isotopically mature crustal material was exposed to erosion. This led to the accelerated influx of radiogenic strontium into the World Ocean. In contrast, the intensification of rift processes and their subsequent conversion into oceanic spreading resulted in the breakup of supercontinents. In the spreading zones, the juvenile isotopically immature mantle matter flew to the surface and interacted with waters of the World Ocean, thus providing the low  $^{87}\text{Sr}/^{86}\text{Sr}$  influx. Alternation of these epochs caused a change of the strontium isotope composition (and  $^{87}\text{Sr}/^{86}\text{Sr}$  values) of seawaters with time.

Following these considerations, we may solve an inverse problem: the available  $^{87}\text{Sr}/^{86}\text{Sr}$  ratio in carbonate rock can be used to estimate its age by the comparison with available data on coeval rocks.

In our case, we may use both  $^{87}\text{Sr}/^{86}\text{Sr}$  data on rocks from definite sections of similar age from different regions of the world (Kaufman et al., 1996; Narbonne, 1994; Brasier et al., 1996; Walter et al., 2000; Pokrovsky et al., 2006, 2020; Sawaki et al., 2008, 2010; Melezhik et al., 2009; Li et al., 2013; Kramchaninov and Kuznetsov, 2014; Pokrovsky and Bujakaite, 2015, 2016; Lan et al., 2019; Kochnev et al., 2018, 2020) and generalized chemostratigraphic curves constructed for the end of Proterozoic, which demonstrate the global  $^{87}\text{Sr}/^{86}\text{Sr}$  variations in carbonate rocks (Halverson et al., 2010; *The Geological ...*, 2012; Pokrovsky et al., 2006, 2012; Kuznetsov et al., 2014; Pokrovsky and Bujakaite, 2016; Xiao et al., 2016; Li et al., 2017). The chemostratigraphic correlations of distal “barren” (devoid of index fossil remains) sections will be more reliable, with allowance for the  $\delta^{13}\text{C}$  variation curves. Examples of these complex chemostratigraphic correlations can be found in (*The Geological ...*, 2012; Gao et al., 2018; Kochnev et al., 2020].

Late Precambrian carbonate sequences (limestones, dolomites) in many regions of the world show wide variations of the carbon and oxygen isotope composition and the strontium isotope ratio (see overview in (Li et al., 2013)).

The Late Neoproterozoic sequences show global positive (545–550 and 560–565 Ma and others (*A Concise ...*, 2016; *Geologic ...*, 2020)) and negative (555 Ma, Shuram (or “Shuram–Wonoka”) (*A Concise ...*, 2016; *Geologic ...*, 2020))  $\delta^{13}\text{C}$  excursions. The carbon and oxygen isotope compositions within these excursions, as well as in the intervals between these global excursions could be significantly shifted (by up to 5‰ and more) in the positive or negative direction. This is for instance typical of carbonate rocks of the Doushantuo Formation (SW China), which lie directly on tillites of the Nantuo Formation (Gao et al., 2018, Fig. 5). The carbonate rocks of the Doushantuo Formation show several sharp positive and negative shifts in  $\delta^{13}\text{C}$  (2–3‰) and  $\delta^{18}\text{O}$  (up to 5‰) even within a single carbonate sequence (e.g., sections of the carbonate sequences of the Ediacaran Doushan-

tuo and Dending formations, Wangji drill core (Gao et al., 2018, Fig. 3)).

Variations (amplitudes of the shift) of  $\delta^{13}\text{C}$  values can also be observed within globally expressed (well correlated between widely spaced sections) excursions. For instance, maximum shifts of these values within a Shuram negative carbon isotope anomaly for carbonates of the Doushantuo Formation, which were formed in the Ediacaran in different facies zones of sedimentation basin, could reach >10‰ (Li et al., 2017, Fig. 3). The amplitudes of  $\delta^{13}\text{C}$  shifts of this anomaly in the Vendian sequences of the southern Siberian Platform show insignificant variations, but almost always decrease to –10‰ and lower (Kochnev et al., 2020).

Thus, in spite of the fact that the Neoproterozoic sequences around the world show significant variations of  $\delta^{13}\text{C}$ , which could be related not only to the global changes of carbon isotope composition of the paleoatmosphere, but also to the paleofacies features of carbonate sedimentation, anomalous excursions occur almost ubiquitously. These excursions serve as stratigraphic markers for the correlation of widely spaced sections.

The studied rocks of the Porozhinsk deposit are closest in age to carbonate rocks of the Pod’emsk Formation from the Chapa River section (Pokrovsky et al., 2012). Carbonate rocks of the Pod’emsk Formation have typical Lower Ediacaran  $^{87}\text{Sr}/^{86}\text{Sr}$  values (0.7076–0.7078) and moderately low  $\delta^{13}\text{C}$  values ( $-1.9 \pm 1.2\text{‰}$ ;  $-3.0\text{‰}$ – $-0.4\text{‰}$  and  $-1.3\text{‰}$ – $-0.6\text{‰}$  in dolomites and limestones, respectively). Based on the isotope characteristics, carbonate rocks of the Pod’emsk Formation developed along the Chapa River significantly differ from the studied dolomites of the Porozhinsk deposit in the Vorogovka trough.

Pokrovsky et al. (2012) believe that the marker carbonate unit in the section of the upper subformation of the Nemchan Formation along the Chapa River can be correlated with the Shuram–Wonoka event. Based on the isotope data ( $^{87}\text{Sr}/^{86}\text{Sr} = 0.7084$ , and  $\delta^{13}\text{C}$  within  $-2.2\text{‰}$ – $-2.5\text{‰}$ ), dolomites from the lower subformation of the Lebyazhino Formation, which overlie the Nemchan Formation along the Chapa River, can be correlated with the transitional Vendian–Cambrian sequences (Nemakit–Daldyn horizon/stage).

Hence, the carbon, oxygen, and strontium ( $^{87}\text{Sr}/^{86}\text{Sr}$ ) isotope data from (Pokrovsky et al., 2012) indicate that dolomites of the Pod’emsk Formation from the Chapa River differ in age from dolomites of the Porozhinsk deposit. We may suggest that the dolomites, which are correlated with the Pod’emsk Formation at the Porozhinsk deposit and have the higher  $^{87}\text{Sr}/^{86}\text{Sr}$  and higher (in general)  $\delta^{13}\text{C}$  values (Fig. 9, Table 1), are much younger than the negative Shuram–Wonoka excursion. In 585–555 Ma carbonates from the type locality of this isotopic carbon excur-



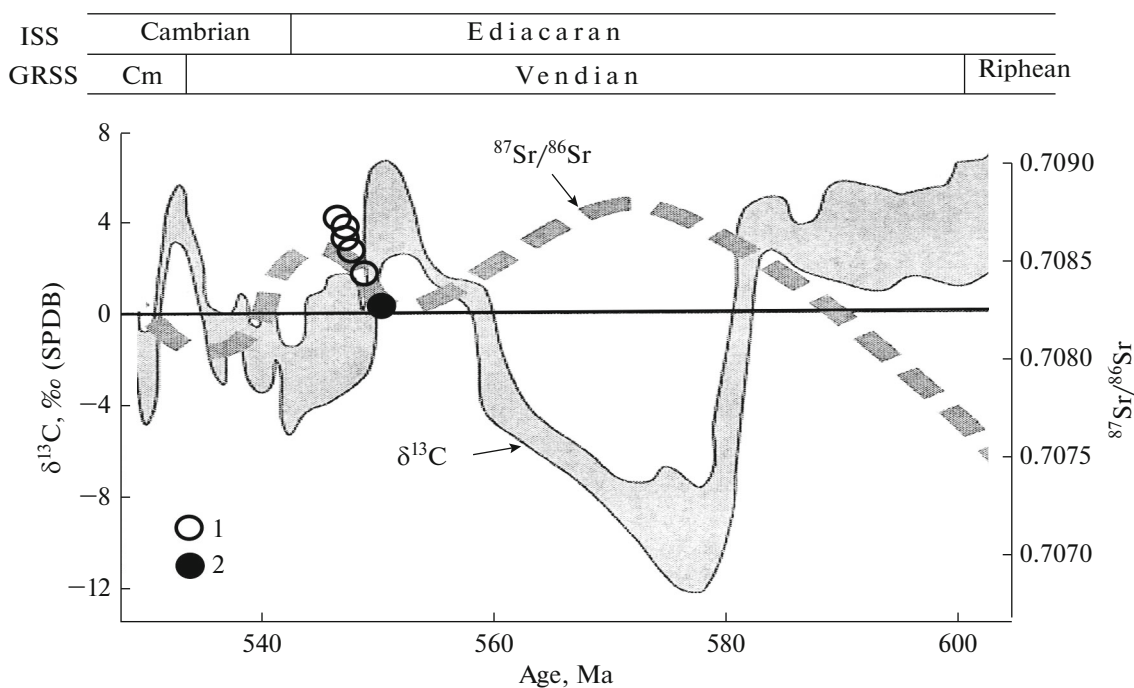


**Fig. 9.** Estimated age of dolomites of the Pod'ensk Formation of the Porozhinsk deposit based on the isotope-geochemical data (modified after (Kochnev et al., 2019). Gray field shows the average  $\delta^{13}\text{C}$  values after (Saltzman and Thomas, 2012). Dashed line shows the average  $^{87}\text{Sr}/^{86}\text{Sr}$  values after (Kuznetsov et al., 2014). (1) shallow dolomites (prospecting trenches, holes, position of symbols is conditionally shown), (2) deep-seated dolomites (200–300 m) from drill cores. Abbreviations: (ISS) International Stratigraphic Scale, (GRSS) General Russian Stratigraphic Scale, (Cm) Cambrian.

sion, the  $\delta^{13}\text{C}$  value decreases to  $-10\text{‰}$  and lower. Thereby, carbonates from this level have the  $^{87}\text{Sr}/^{86}\text{Sr}$  ratio varying within 0.7080–0.7090 (Xiao et al., 2016).

To roughly date the studied dolomites of the Porozhinsk deposit, we attempted to solve the inverse problem: to estimate their age by comparison of the obtained  $^{87}\text{Sr}/^{86}\text{Sr}$  and  $\delta^{13}\text{C}$  values with available data on the Vendian (Ediacaran) rocks. The most complete and representative (at present)  $^{87}\text{Sr}/^{86}\text{Sr}$  variation curves for Neoproterozoic is the Sr-chemostratigraphic curve presented in (Kuznetsov et al., 2014). We used this curve in combination with the  $\delta^{13}\text{C}$  variation curve for the end of Neoproterozoic (Kochnev et al., 2019).

Figure 9 shows the position of the obtained isotope ( $^{87}\text{Sr}/^{86}\text{Sr}$ ,  $\delta^{13}\text{C}$ ) data on dolomites of the Porozhinsk dolomites. It is seen that the isotope characteristics of the studied dolomites are restricted to the “ascending” branch of the second positive  $^{87}\text{Sr}/^{86}\text{Sr}$  peak corresponding to the end of Ediacaran (Late Vendian) in the generalized Sr-chemostratigraphic curve (Kuznetsov et al., 2014). This means that the studied dolomites of the Porozhinsk deposit are younger than dolomites of the Pod'ensk Formation from the Chapa River section (Pokrovsky et al., 2012).

It should also be noted that the lowest values are usually taken as the initial  $^{87}\text{Sr}/^{86}\text{Sr}$  (as, for example, for Neoproterozoic sequences in China, Morocco,

Mongolia, and Siberia (Li et al., 2013)). Therefore, the lowest  $^{87}\text{Sr}/^{86}\text{Sr}$  values obtained for the deepest dolomites in the Porozhinsk deposit (0.70822–0.70827) are representative and correspond to the strontium isotope ratio in seawater at the end of Neoproterozoic.

At the same time the higher  $^{87}\text{Sr}/^{86}\text{Sr}$  ratios also could be representative, as they could be related not only with the secondary transformation of initial rocks, but also with the increase of this ratio (as other chemical and isotope characteristics) in the paleohydrosphere during the geological evolution of the crust and hydrosphere.

This assumption is confirmed by the carbon and oxygen isotope data. As was shown above and in (Kuleshov et al., 2021), the studied dolomites of the Porozhinsk deposit were formed in marine sedimentation basins, which differed in the oxygen isotope composition of seawater and/or in temperature. The dolomites also differ in  $\text{Ce}^*/\text{Ce}_{\text{NASC}}$  anomalies. Therefore, we may suggest that the higher  $^{87}\text{Sr}/^{86}\text{Sr}$  ratio in shallow dolomites of the Porozhinsk deposit (0.70840–0.70864) also could be close to the initial values and reflect the strontium isotope ratios in seawater by the end of Ediacaran.

Thus, the manganese ore formation at the Yenisei Ridge could be younger than previously inferred by some researchers (Mstislavsky and Potkonen, 1990) and can be related to the Late Vendian manganese ore

sedimentation basins (Golovko et al., 1982; Tsykin et al., 1987; Tsykin and Sviridov, 2012).

## CONCLUSIONS

Based on the obtained strontium isotope data and their distribution in carbonate rocks and ores of the Porozhinsk deposit, the following conclusions can be drawn:

(1) Carbonate rocks and ores of the Porozhinsk deposit show a wide scatter of  $^{87}\text{Sr}/^{86}\text{Sr}$  within 0.70825–0.70924. These data in combination with carbon ( $\delta^{13}\text{C} = -14.6\text{...}2.0\text{‰}$ , PDB) and oxygen ( $\delta^{18}\text{O} = 19.4\text{...}28.3\text{‰}$ , SMOW) isotope variations indicate different formation conditions and sources of the studied rocks.

(2) The  $^{87}\text{Sr}/^{86}\text{Sr}$  values in dolomites of the Porozhinsk deposit are much higher than those in the carbonate rocks (dolomites, limestones) of the Pod’emsk Formation from the Chapa River section (Chapa–Teya trough). This indicates different ages of dolomites from these areas.

(3) Position of  $^{87}\text{Sr}/^{86}\text{Sr}$  composition points of dolomites from the Porozhinsk deposit on the  $^{87}\text{Sr}/^{86}\text{Sr}$  secular variation curve for the Late Proterozoic oceans (Kuznetsov et al., 2014) suggests that the dolomite sequence of the Porozhinsk deposit is younger than the carbonates of the Pod’emsk Formation from the Chapa River section (Chapa–Teya trough).

(4) The Mn/Sr ratio usually applied as the geochemical criterion of secondary alteration of carbonates (for interpretation of the  $^{87}\text{Sr}/^{86}\text{Sr}$  ratio and selection of the least altered material for chemostratigraphic considerations) is not suitable for rocks formed in the Mn-bearing sedimentation basin of the Porozhinsk deposit (Yenisei Ridge).

## ACKNOWLEDGMENTS

We are grateful to G.V. Gorshkov and E.G. Pilipchuk for consultation on the geology of the Porozhinsk deposit and invaluable help in the sampling.

## FUNDING

This work was supported by the Presidium of the Russian Academy of Sciences (program no. 1.48) and carried out under the government-financed research project of the Geological Institute of the Russian Academy of Sciences. Field works in the northern Yenisei Ridge were financially supported by the Russian Foundation for Basic Research (project no. 19-05-00794). Accumulation and systematization of the chemostratigraphic data on the Siberian Platform and surrounding old orogenic structures were financially supported by the Ministry of Education and Science of the Russian Federation (Megaproject no. 075-15-2019-

1883 “Orogenesis: Formation and Growth of Continents and Supercontinents”).

## CONFLICT OF INTEREST

The authors declare that they have no conflicts of interest.

## REFERENCES

- A Concise Geologic Time Scale*, Ogg, J.G., Ogg, G., and Gradstein, F.M., Eds, Amsterdam, Tokio: Elsevier, 2016.
- Brasier, M.D., Shields, G., Kuleshov, V.N., and Zhegalo, E.A., Integrated chemo- and biostratigraphic calibration of early animal evolution: Neoproterozoic–early Cambrian of south-west Mongolia, *Geol. Mag.*, 1996, vol. 133, no 1/4, pp. 445–485.
- Degens, E.T., *Geochemistry of Sediments. A Brief Survey*, New Jersey: Prentice-Hall, 1965. Translated under the title *Geokhimiya osadochnykh obrazovaniy*, Moscow: Mir, 1967.
- Degens, E.T., Distribution of stable isotopes in carbonates, in *Karbonatnye porody: fiziko-khimicheskaya kharakteristika i metody issledovaniya* (Carbonate Rocks: Physicochemical Characteristics and Methods of Study), Chilingar, J., et al., Eds., Moscow: Mir, 1971, pp. 141–153.
- Faure, G., *Principles of Isotope Geology*, New York: Wiley, 1986. Translated under the title *Metody izotopnoi geologii*, Moscow: Mir, 1989.
- Friedman, J. and O’Neil, Y.R., *Compilation of Stable Isotope Fractionation Factors of Geochemical Interest*, Wash. (D.C.) Gov. Print. Off., 1977.
- Gao, Y., Zhang, X., Zhang, G., et al., Ediacaran negative C-isotopic excursions associated with phosphogenic events: evidence from South China, *Precambrian Res.*, 2018, vol. 307, pp. 218–228.
- Geologic Time scale*, Gradstein, F.M., Ogg, J.G., Schmitz, M.D., and Ogg G.M., Eds., Amsterdam: Elsevier, 2020, vol. 1.
- Golovko, V.A. and Nasedkina, V.Kh., The composition and genesis of manganese ores in the Porozhinsk deposit (Yenisei Ridge), in *Geologiya i geokhimiya margantsa* (Geology and Geochemistry of Manganese), Moscow: Nauka, 1982, pp. 104–109.
- Golovko, V.A., Mstislavskii, M.M., Nasedkina, V.Kh., et al., The Precambrian manganese potential of the Yenisei Ridge, in *Geologiya i geokhimiya margantsa* (Geology and Geochemistry of Manganese), Moscow: Nauka, 1982, pp. 94–104.
- Gorshkov, G.V., The Porozhinsk manganese ore deposit, *Otechestv. Geol.*, 1994, no. 10, pp. 58–61.
- Gosudarstvennyi doklad “O sostoyanii i ispol’zovanii mineral’no-syr’evykh resursov Rossiiskoi Federatsii v 2018 godu”* (State Report on “State and Use of Raw Mineral Resources in the Russian Federation in 2018”), Moscow: Min. Prirodn. Resurs. Ekol. RF, 2019.
- Halverson, G.P., Wade, B.P., Hurtgen, M.T., and Barovich, K.M., Neoproterozoic chemostratigraphy, *Precambrian Res.*, 2010, vol. 182, pp. 337–350.
- Kaufman, A.J., Jacobsen, S.B., and Knoll, A.H., The Vendian record of Sr and C isotopic variations in seawater: implications for tectonics and paleoclimate, *Earth Planet. Sci. Lett.*, 1993, vol. 120, no. 3, pp. 409–430.
- Kaufman, A.J. and Knoll, A.H., Neoproterozoic variations in the C-isotopic composition of seawater: stratigraphic and

- biogeochemical implications, *Precambrian Res.*, 1995, vol. 73, pp. 27–49.
- Kaufman, A.J., Knoll, A.H., Semikhatov, M.A., et al., Integrated chronostratigraphy of Proterozoic–Cambrian boundary beds in the western Anabar region, northern Siberia, *Geol. Mag.*, 1996, vol. 133, pp. 509–533.
- Khabarov, E.M., Ponomarchuk, V.A., and Morozova, I.P., Strontium isotopic evidence for supercontinental breakup and formation in the Riphean: Western margin of the Siberian Craton, *Russ. J. Earth Sci.*, 2002, vol. 4, no. 4, pp. 259–269.
- Khabarov, E.M. and Izokh, O.P., Sedimentology and isotope geochemistry of Riphean carbonate rocks in the Kharaulakh Uplift in northern part of Eastern Siberia, *Geol. Geofiz.*, 2014.
- Khomentovskii, V.V., The Angarian in the Yenisei Ridge: A standard Neoproterozoic unit, *Geol. Geofiz.*, 2015, vol. 55, no. 3, pp. 464–472.
- Khomentovskii, V.V., Shenfel, V.Yu., Yakshin, M.S., and Butakov, E.P., *Opornye razrezy otlozhenii verkhnego dokembriya i nizhnego kembriya Sibirskoi platformy* (Reference Sections of the Upper Precambrian and Lower Cambrian Rocks in the Siberian Platform), Moscow: Nauka, 1972.
- Kirichenko, G.I., Late and postgeosynclinal troughs in the Yenisei Ridge and adjacent Baikallide regions, *Sov. Geol.*, 1965, no. 7, pp. 18–35.
- Kochnev, B.B., Pokrovskii, B.G., Kuznetsov, A.B., and Marusin, V.V., The C- and Sr-isotope chemostratigraphy of Vendian–Lower Cambrian carbonate rocks in central regions of the Siberian Platform, *Geol. Geofiz.*, 2018, vol. 59, no. 6, pp. 731–755.
- Kochnev, B.B., Kuznetsov, A.B., Pokrovsky, B.G., Sitkina, D.R., and Smirnova, Z.B., C and Sr isotope chemostratigraphy and Pb–Pb age of carbonate deposits of the Vorogovka Group (Neoproterozoic), northwest of the Yenisei Range, *Stratigr. Geol. Correl.*, 2019, vol. 27, no. 5, pp. 553–575.
- Kochnev, B.B., Proshenkin, A.I., Pokrovskii, B.G., and Letnikova, E.F., The Vendian Taseev Group at the southwestern margin of the Siberian Platform: Isotope-geochemical and geochronological data, age, and, correlation, *Geol. Geofiz.*, 2020, vol. 61, no. 10, pp. 1370–1385.
- Kramchaninov, A.Yu. and Kuznetsov, A.B., Variations of  $\delta^{88}\text{Sr}$  and  $^{87}\text{Sr}/^{86}\text{Sr}$  in Neoproterozoic sedimentary carbonates (the Tsagaan Oolom Formation, West Mongolia), *Dokl. Earth Sci.*, 2014, vol. 455, no. 4, pp. 414–418.
- Kuleshov, V.N., Isotope compositions ( $\delta^{13}\text{C}$ ,  $\delta^{18}\text{O}$ ) of manganese carbonates of the Porozhinsk deposit (Yenisei Ridge, Krasnoyarsk region), *Lithol. Miner. Resour.*, 2018, no. 6, pp. 525–533.
- Kuleshov, V.N. and Zhegallo, E.A., Carbon and oxygen isotopic compositions in the Vendian–Cambrian carbonate rocks of western Mongolia, *Lithol. Miner. Resour.*, 1997, no. 1, pp. 41–49.
- Kuleshov, V.N., Sviridov, L.I., and Petrov, O.L., Specific features of the genesis of manganese carbonates in the Porozhinsk deposit (Yenisei Ridge, Krasnoyarsk region), *Lithol. Miner. Resour.*, 2021, no. 3, pp. 248–265.
- Kuleshov, V.N., Bychkov, A.Yu., and Sviridov, L.I., Specific features of the rare earth element distribution in rocks and ores of the Porozhinsk manganese deposit (Yenisei Ridge, Krasnoyarsk region), *Lithol. Miner. Resour.*, 2022, no. 4, pp. 209–313.
- Kuznetsov, A.B., Semikhatov, M.A., and Gorokhov, I.M., The Sr isotope composition of the World Ocean, marginal and inland seas: Implications for the Sr isotope stratigraphy, *Stratigr. Geol. Correl.*, 2012, vol. 20, no. 6, pp. 501–515.
- Kuznetsov, A.B., Semikhatov, M.A., and Gorokhov, I.M., The Sr isotope chemostratigraphy as a tool for solving stratigraphic problems of the Upper Proterozoic (Riphean and Vendian), *Stratigr. Geol. Correl.*, 2014, vol. 22, no. 6, pp. 553–575.
- Kuznetsov, N.B., Rud'ko, S.V., Shatsillo, A.V., and Rud'ko, D.V., New finds of ichofossils from the Vendian/Cambrian boundary levels at the western periphery of the Siberian Platform (field works in 2017), in *Geodinamicheskaya evolyutsiya litosfery Tsentral'no-Aziatskogo podvizhnogo poyasa (ot okeana k kontinentu)* (Geodynamic Evolution of Lithosphere in the Central Asian Mobile Belt: From the Ocean to Continent), Irkutsk: IZK SO RAN, 2017, pp. 153–155.
- Kuznetsov, N.B., Priyatkina, N.S., Rud'ko, S.V., et al., Primary data on U/Pb-isotope ages and Lu/Hf-isotope geochemical systematization of detrital zircons from the Lopatinskii Formation (Vendian–Cambrian transition levels) and the tectonic nature of Teya–Chapa Depression (northeastern Yenisei Ridge), *Dokl. Earth Sci.*, 2018, vol. 479, no. 1, pp. 286–289.
- Lan, Zh., Sano, Y., Yahagi, T., et al., An integrated chemostratigraphic ( $\delta^{13}\text{C}$ – $\delta^{18}\text{O}$ – $^{87}\text{Sr}/^{86}\text{Sr}$ – $\delta^{15}\text{N}$ ) study of the Doushantuo Formation in western Hubei Province, South China, *Precambrian Res.*, 2019, vol. 320, pp. 232–252.
- Li, D., Linga, H.-F., Shields-Zhou, G.A., et al., Carbon and strontium isotope evolution of seawater across the Ediacaran–Cambrian transition: evidence from the Xiaotan section, NE Yunnan, South China, *Precambrian Res.*, 2013, vol. 225, pp. 128–147.
- Li, C., Hardisty, D.S., Luo, G., et al., Uncovering the spatial heterogeneity of Ediacaran carbon cycling, *Geobiology*, 2017, vol. 15, no. 2, pp. 211–224.
- Melezhik, V.A., Pokrovsky, B.G., and Fallick, A., E et al., Constraints on the  $^{87}\text{Sr}/^{86}\text{Sr}$  of Late Ediacaran seawater: insights from high-Sr limestones, *J. Geol. Soc. Lon.*, 2009, vol. 166, pp. 183–191.
- Mkrtych'yan, A.K., Tsykin, R.A., and Savan'yak, Yu.V., Manganese potential of the Yenisei Ridge, in *Novye dannye po margantsevym mestorozhdeniyam SSSR* (New Data on Manganese Deposits in the Soviet Union), Sapozhnikov, D.G., Ed., Moscow: Nauka, 1980.
- Mstislavskii, M.M. and Potkonen, N.I., The Porozhinsk manganese deposit in the Yenisei Ridge, *Geol. Rudn. Mestorozhd.*, 1990, no. 3, pp. 82–95.
- Narbonne, G.M., Kaufman, A.J., and Knoll, A.H., Integrated chemostratigraphy and biostratigraphy of the upper Windermere Supergroup (Neoproterozoic), northwestern Canada: implications for Neoproterozoic correlations and the early evolution of animals, *Geology*, 1994, vol. 106, no. 10, pp. 1281–1292.
- Nozhkin, A.D., Postnikov, A.A., Nagovitsin, K.E., et al., The Neoproterozoic Chingasan Group in the Yenisei Ridge: New data on the age and formation conditions, *Geol. Geofiz.*, 2007, vol. 48, no. 12, pp. 1307–1320.
- Podkovyrov, V.N., Semikhatov, M.A., Kuznetsov, A.B., et al., Carbonate carbon isotopic composition in the Upper Riphean stratotype, the Karatau Group, southern Urals, *Stratigr. Geol. Correl.*, 1998, vol. 6, no. 4, pp. 319–335.

- Pokrovsky, B.G. and Bujakaite, M.I., Geochemistry of C, O, and Sr isotopes in the Neoproterozoic carbonates from the southwestern Patom paleobasin, southern middle Siberia, *Lithol. Miner. Resour.*, 2015, no. 2, pp. 14–169.
- Pokrovsky, B.G. and Bujakaite, M.I., Isotopic compositions of C, O, Sr, and S and problem of ages of the Katera and Uakit groups, western Transbaikal region, *Lithol. Miner. Resour.*, 2016, no. 4, pp. 262–282.
- Pokrovsky, B.G., Melezhik, V.A., and Bujakaite, M.I., Carbon, oxygen, strontium, and sulfur isotopic compositions in Late Precambrian rocks of the Patom Complex, Central Siberia: Communication 1. Results, isotope stratigraphy, and dating problems, *Lithol. Miner. Resour.*, 2006, no. 5, pp. 450–474.
- Pokrovsky, B.G., Bujakaite, M.I., and Kokin, O.V., Geochemistry of C, O, and Sr isotopes and chemostratigraphy of Neoproterozoic rocks in the northern Yenisei Ridge, *Lithol. Miner. Resour.*, 2012, no. 2, pp. 177–199.
- Pokrovsky, B.G., Bujakaite, M.I., Petrov, O.L., and Koleznikova, A.A., The C, O, and Sr isotope chemostratigraphy of the Vendian (Ediacaran)–Cambrian transition, Olekma River, western slope of the Aldan Shield, *Stratigr. Geol. Correl.*, 2020, vol. 28, no. 5, pp. 479–492.
- Priyatkina, N., Collins, W.J., Khudoley, A.K., et al., Detrital zircon record of Meso- and Neoproterozoic sedimentary basins in northern part of the Siberian Craton: characterizing buried crust of the basement, *Precambrian Res.*, 2016, vol. 285, pp. 21–38.
- Rud'ko, S., Kuznetsov, N., Shatsillo, B., et al., Sturtian glaciation in Siberia: evidence of glacial origin and U–Pb dating of the diamictites of the Chivida Formation in the north of the Yenisei Ridge, *Precambrian Res.*, 2020, vol. 345.  
<https://doi.org/10.1016/j.precamres.2020.105778>
- Rud'ko, S.V., Kuznetsov, A.B., and Petrov, P.Yu., Strontium isotope composition in limestones of the Dal'nyaya Taiga Group in the Patom Basin: Vendian reference section of Siberia, *Lithol. Miner. Resour.*, 2020, no. 3, pp. 206–217.
- Sawaki, Y., Ohno, T., Fukushi, Y., et al., Sr isotope excursion across the Precambrian–Cambrian boundary in the Three Gorges area, South China, *Gondwana Res.*, 2008, vol. 14, pp. 134–147.
- Sawaki, Y., Ohno, T., Tahata, M., et al., The Ediacaran radiogenic Sr isotope excursion in the Doushantuo Formation in the Three Gorges area, South China, *Precambrian Res.*, 2010, vol. 176, pp. 46–64.
- Semikhatov, M.A., *Rifei i nizhnii kembrii Eniseiskogo kryazha* (Riphean and Lower Cambrian in the Yenisei Ridge), Moscow: AN SSSR, 1962.
- Semikhatov, M.A., Kuznetsov, A.B., Podkovyrov, V.N., et al., The Yudoma Group of stratotype area: C-isotope chemostratigraphic correlations and Yudomian–Vendian relation, *Stratigr. Geol. Correl.*, 2004, vol. 12, no. 5, pp. 435–455.
- Semikhatov, M.A., Kuznetsov, A.B., Maslov, A.V., et al., Stratotype of the Lower Riphean, the Burzyan Group of the Southern Urals: Lithostratigraphy, paleontology, geochronology, Sr- and C-isotopic characteristics of its carbonate rocks, *Stratigr. Geol. Correl.*, 2009, vol. 17, no. 6, pp. 574–601.
- Shatsillo, A.V., Kuznetsov, N.B., Pavlov, V.E., et al., The first magnetostratigraphic data on the stratotype of the Lopata Formation, Northeastern Yenisei Ridge: Problems of its age and paleogeography of the Siberian Platform at the Proterozoic–Phanerozoic boundary, *Dokl. Earth Sci.*, 2015, vol. 465, no. 4, pp. 1211–1214.
- Sovetov, Yu.K., *Verkhnedokembriiskie peschaniki yugo-zapada Sibirskoi platformy* (Upper Precambrian Sandstones in the Southwestern Siberian Platform), Novosibirsk: Nauka, 1977.
- Sovetov, J.K. and Blagovidov, V.V., The shelf sedimentation at the late stage of the Vorogovka trough development, Yenisei Ridge, *Geol. Geofiz.*, 1996, vol. 37, no. 4, pp. 45–51.
- Sovetov, J.K. and Blagovidov, V.V., Reconstruction of the sedimentation basin: Example from the Vendian foredeep in the southwestern Siberian Platform, in *Osadochnye basseiny: metodika izucheniya, stroenie i evolyutsiya* (Oceanic Basins, Study Methods, Structure, and Evolution), Moscow: Nauchn. Mir, 2004.
- Sovetov, J.K. and Le Heron, D.P., Birth and evolution of a Cryogenian basin: glaciation, rifting and sedimentation in the Vorogovka Basin, Siberia, *Sedimentology*, 2016, vol. 63, pp. 498–522.
- The Geologic Time scale*, Gradstein, F.M., Ogg, J.G., Schmitz, M.D. and Ogg, G.M., Eds, Amsterdam: Elsevier, 2012.
- Tsykin, R.A., The stagewise formation of the Porozhinsk manganese deposit (Yenisei Ridge), in *Petrologiya i poleznye iskopaemye Krasnoyarskogo kraya* (Petrology and Mineral resources in the Krasnoyarsk Region), Novosibirsk: Nauka, 1984, pp. 99–104.
- Tsykin, R.A., Specific features of the Mesozoic–Cenozoic hypergenesis in the Porozhinsk manganese ore area (Yenisei Ridge), *Geol. Rudn. Mestorozhd.*, 1992, vol. 34, no. 5, pp. 73–79.
- Tsykin, R.A. and Sviridov, L.I., Composition and formation conditions of the manganese member in the Upper Riphean Pod'em Formation (Yenisei Ridge), *Litol. Polezn. Iskop.*, 1993, no. 5, pp. 27–33.
- Tsykin, R.A. and Sviridov, L.I., *Porozhinskii margantsenonnyi uzel: monografiya* (The Porozhinsk Manganese Node: Monography), Krasnoyarsk: Sibir. Feder. Univ., 2012.
- Tsykin, R.A., Sviridov, L.I., and Kostenenko, L.P., Manganese ores in the Mokhovoe deposit (Yenisei Ridge), *Geol. Rudn. Mestorozhd.*, 1987, no. 1, pp. 112–117.
- Ustalov, V.V., Structures, formations, and manganese potential of the Vorogovka trough (Yenisei Ridge), *Extended Abstract of PhD (Geol.–Miner.) Dissertation*, Moscow: MGU, 1982.
- Vinogradov, V.I. and Chernyshev, I.V., Standard specimens and reference samples for the isotope-geochemical studies, *Izv. AN. SSSR, Ser. Geol.*, 1987, no. 1, pp. 71–78.
- Vishnevskaya, I.A., Letnikova, E.F., Proshenkin, A.I., et al., The Vendian Vorogovka Group in the Yenisei Ridge: Chemostratigraphy and results of U–Pb dating of detrital zircons, *Dokl. Earth Sci.*, 2017, vol. 476, no. 1, pp. 1010–1015.
- Xiao, Sh., Narbonne, G.M., and Zhou, Ch., Towards an Ediacaran time scale: problems, protocols, and prospects, *Episodes*, 2016, vol. 39, no. 4, pp. 540–555.
- Walter, M.R., Veeres, J.J., Calver, C.R., et al., Dating the 840–544 Ma Neoproterozoic interval by isotopes of strontium, carbon and sulfur in seawater and some interpretative models, *Precambrian Res.*, 2000, vol. 100, pp. 371–433.

Translated by M. Bogina